

CHAOTIC DOUBLE CYCLING

ALEXANDRE A.P. RODRIGUES, ISABEL S. LABOURIAU, AND MANUELA A.D. AGUIAR

ABSTRACT. We study the dynamics of a generic vector field in the neighbourhood of a heteroclinic cycle of non-trivial periodic solutions whose invariant manifolds meet transversely. The main result is the existence of chaotic double cycling: there are trajectories that follow the cycle making any prescribed number of turns near the periodic solutions, for any given bi-infinite sequence of turns. Using symbolic dynamics, arbitrarily close the cycle, we find a robust and transitive set of initial conditions whose trajectories follow the cycle for all time and that is conjugate to a Markov shift over a finite alphabet. This conjugacy allows us to prove the existence of infinitely many heteroclinic and homoclinic subsidiary connections, which give rise to a heteroclinic network with infinitely many cycles and chaotic dynamics near them, exhibiting themselves switching and cycling. We construct an example of a vector field with Z_3 symmetry in a 5-dimensional sphere with a heteroclinic cycle that has this property.

1. INTRODUCTION

A particularly important subject in the theory of nonlinear dynamical systems is the study of the behaviour near homoclinic and heteroclinic cycles. There are several studies of the homoclinic and heteroclinic issues in the settings of symmetry (Field [14], Krupa [25], [26] and Aguiar *et al* [4], [5]), coupled cell systems (Aguiar *et al* [2]), Hamiltonian systems (Homburg *et al* [20]) and reversible systems (Lamb *et al* [28]). A review of homoclinic and heteroclinic theory for autonomous vector fields is given in Homburg *et al* [21].

Roughly speaking, a homoclinic trajectory in a dynamical system defined by an ordinary differential equation is a solution bi-asymptotic to an invariant set and a heteroclinic connection is a solution asymptotic to different invariant sets for $t \rightarrow -\infty$ and for $t \rightarrow +\infty$. Here we are interested in the case where those invariant sets are hyperbolic non-trivial periodic solutions. We shall think of a heteroclinic cycle as a set of invariant sets (which we will call nodes) connected in a cycle of heteroclinic orbits. A heteroclinic network is a connected set of heteroclinic cycles.

Heteroclinic orbits often arise when a system may cycle through many states in models of physical systems with symmetry (see for example Armbruster [7] or Melbourne *et al* [30]). Symmetry is a natural setting for persistent heteroclinic cycles. In this context, Krupa *et al* [27] give a sufficient condition (also necessary when some additional conditions are satisfied) for a heteroclinic cycle to be asymptotically stable: trajectories near the heteroclinic cycle will follow and approach it infinitely.

Associated to asymptotically stable heteroclinic cycles we observe intermittency: trajectories near the heteroclinic cycle spend some time near each node and then jump to the next one. These trajectories follow the connections around the cycle, returning to each node infinitely many times. Moreover, the trajectories spend more and more time near the nodes on each visit. For a given trajectory approaching the cycle, the duration of visits is a geometrically increasing sequence of times.

A natural question arises: is it possible to control the time on each visit to a neighbourhood of the nodes of the cycle?

If the cycle is asymptotically stable, the answer has been given by Melbourne [29]. If the invariant manifolds of the nodes meet transversely, the cycle is not asymptotically stable, the system is chaotic and there are few results concerning the dynamic behaviour in the neighbourhood of the cycle.

2000 *Mathematics Subject Classification.* Primary: 37C29; Secondary: 34E10, 34C28, 37C27, 37C20.

Key words and phrases. vector fields, heteroclinic cycle and networks, bi-infinite cycling, symbolic dynamics, horseshoe in time.

The research of all authors at Centro de Matemática da Universidade do Porto (CMUP) had financial support from Fundação para a Ciência e a Tecnologia (FCT), Portugal, through the programs POCTI and POSI with European Union and national funding. A.A.P. Rodrigues was supported by the grant SFRH/BD/28936/2006 of FCT.

In this paper, we provide an affirmative answer to the question in the context of non-asymptotically stable heteroclinic cycles between non-trivial periodic solutions, by counting the number of times a trajectory turns around each node.

Given a set of neighbourhoods of the nodes and any prescribed number of turns inside each of the neighbourhoods, we prove the existence of a trajectory that follows the cycle making the prescribed turns as it travels along the cycle. The number of turns may be chosen as an arbitrary bi-infinite sequence of numbers. This is not a temporal transient phenomenon; it is a robust behaviour that we call chaotic double cycling.

The study of this specific type of chaotic dynamics plays an important role in several applied subjects, for instance in biomedical rhythms (Savi [39]) and cryptography (Palacios [35]).

In the Hamiltonian setting this has been studied in the context of the two and three-body problems by Moeckel [31] and by Koon *et al* [24]. Both papers prove the existence of homoclinic and heteroclinic cycles between two periodic solutions which have the same energy for a Hamiltonian vector field. Using the terminology of Aguiar *et al* [5], they show the existence of switching near the cycle (trajectories follow the cycles in any possible order of heteroclinic connections). Moeckel [31] argues for chaotic changes of configuration in a five-dimensional submanifold of the twelve-dimensional configuration space. For a set of spherical neighbourhoods of the cycle, Koon *et al* prove the existence of trajectories rotating any number of times near each periodic solution. One of the key ingredients in the proof, as in our case, is the transversality of the invariant manifolds. However, the restriction of a Hamiltonian system to an energy level does not define a generic differential equation — for instance, its flow preserves volume. The dynamical issues addressed by Moeckel are different from ours. In particular they do not discuss cycling, which is the main point of this article.

A heteroclinic cycle cannot be asymptotically stable if it is part of a heteroclinic network. In this case, the cycle may attract a great part or almost all the points in its neighbourhood but not all of them. In [37], Postlethwaite *et al* report interesting cycling behaviour around cycles in a robust heteroclinic network of equilibria. They conclude that the sequence of loops around each cycle can be either constant or aperiodic. That is what they call regular and irregular cycling, respectively. However, the time spent near each equilibrium increases in both cases.

We show cycling with chaotic behaviour, even though the nodes in the heteroclinic cycles we consider are not chaotic sets. This differs from the situation studied in Dellnitz *et al* [13], where cycling chaos is proved for heteroclinic cycles whose nodes are chaotic attractors. For robust cycling between chaotic sets, see also Ashwin *et al* [11]. The system in [13] corresponds to a network of three identical coupled cell systems of differential equations. In [34], Palacios shows that cycling chaos can also occur for coupled systems of difference equations, and Palacios *et al* [36] address the generalization of cycling behaviour to networks of more than three near-identical cell systems.

We study the dynamics near a cycle of periodic solutions, first in a 3-dimensional manifold, then in any dimension. We ask for transverse intersection of invariant manifolds of all successive nodes. This is only possible because the heteroclinic cycle contains periodic trajectories and not equilibria.

After some preliminary definitions in section 2, the proof in 3 dimensions occupies sections (3-5): notation and definitions in section 3; results that prepare the proof in section 4.

The main point of the proof given in section 5 is to find a set Λ of initial conditions whose trajectories remain near the cycle for all time and whose behaviour may be coded using symbolic dynamics. However, our coding is not only related to the space orbit of the associated trajectory, but also to the number of times that the trajectory cycles around each node, like a horseshoe in time.

The construction of Λ and of the coding is done in two steps. First, we obtain a set $\Lambda_{\mathbf{N}}$ where we code the dynamics by the number of turns made by a trajectory around each node. The dynamics is conjugated to a shift acting on sequences from an infinite symbol set. This establishes the cycling. The second step is to find another set Λ of initial conditions for nonwandering trajectories where the dynamics may be coded by sequences on a finite set of symbols. Although the construction of Λ may be done directly and cycling may be obtained directly from the second coding, the geometry for the direct coding is more intricate, so we have chosen this roundabout way for the sake of clarity.

The coding by a finite set of symbols allows us to obtain further results on the dynamics, presented in section 6. In particular we prove the existence of infinitely many subsidiary homoclinic and heteroclinic connections near the original cycle. Each new cycle may exhibit persistent cycling, giving rise to a very

complicated heteroclinic network. This leads to horseshoe dynamics (in space) conjugated to a Markov shift near any cycle in the network, including the original one. The use of symbolic dynamics allows us to conclude other properties of the invariant set, such as topological mixing and the existence of a Gibbs measure (under the restrictions presented by Sarig [38]).

The extension of our results to higher dimensions is proved in section 7, where we use the center manifold theorem for heteroclinic cycles studied by Shaskov *et al* [40] (in the context of homoclinic orbits) and Shilnikov *et al* [41]. Under some generic hypothesis, we reduce the study of the dynamics near a heteroclinic cycle in an n -dimensional manifold, to a 3-dimensional flow-invariant centre manifold containing the cycle.

We end by presenting the construction of an example of a system of differential equations with \mathbf{Z}_3 symmetry in a 5-dimensional globally attracting sphere in \mathbf{R}^6 , whose flow has a heteroclinic cycle between three periodic solutions. We show numerical evidence that the invariant manifolds meet transversely and that thus the example satisfies the conditions of the result and chaotic cycling holds. This last property is illustrated by numerical plots of solutions to the equations.

2. PRELIMINARIES

Let M be a smooth n -dimensional manifold and let $f : M \rightarrow TM$ be a smooth vector field defined on M . Denote by $\phi(t, p)$ the unique solution $x(t)$ of the initial value problem:

$$(1) \quad \dot{x} = f(x), \quad x(0) = p.$$

In this paper we consider non-trivial periodic solutions of (1) that are hyperbolic and that have at least one Floquet multiplier with absolute value greater than 1 and at least one Floquet multiplier with absolute value less than 1. We call these *periodic solutions of saddle type*.

Given two periodic solutions c_i and c_j of (1) of saddle type, a heteroclinic connection from c_i to c_j is a trajectory contained in $W^u(c_i) \cap W^s(c_j)$ that will be denoted $[c_i \rightarrow c_j]$.

Let $\mathcal{S} = \{c_j : j \in \{1, \dots, k\}\}$ be a finite ordered set of periodic solutions of saddle type of (1) such that

$$\forall j \in \{1, \dots, k\} \quad W^u(c_j) \cap W^s(c_{j+1}) \neq \emptyset \pmod{k}.$$

A *heteroclinic cycle* Σ associated to \mathcal{S} is the union of the saddles in \mathcal{S} with a heteroclinic connection $[c_j \rightarrow c_{j+1}] \pmod{k}$, for each $j \in \{1, \dots, k\}$. If $k = 1$, the heteroclinic cycle is called *homoclinic* cycle. We denote by $\Sigma = \langle c_1, \dots, c_k \rangle$ a heteroclinic cycle associated to $\{c_j : j \in \{1, \dots, k\}\}$ and we refer to the saddles defining the heteroclinic cycle as *nodes*. A *heteroclinic network* is a connected set that is the union of heteroclinic cycles.

Given a heteroclinic cycle of periodic solutions Σ with nodes c_j , $j = 1, \dots, k$, let V_Σ be a compact neighbourhood of Σ and let V_j be pairwise disjoint compact neighbourhoods of the nodes $c_j \in \mathcal{S}$, such that each boundary ∂V_j is a finite union of smooth manifolds with boundary, that are transverse to the vector field everywhere, except for their boundary. Then each V_i is called an *isolating block for c_i* and $\mathcal{V} = \{V_i\}_{i \in \{1, \dots, k\}}$ is called a *system of isolating blocks for Σ* .

For each $V_j \in \mathcal{V}$, consider a codimension 1 submanifold with boundary $\Pi_j \subset V_j$ of M , such that:

- the flow is transverse to Π_j ;
- Π_j intersects ∂V_j transversely;
- $\Pi_j \cap c_j$ has only one element.

We call Π_j a *counting section*. Any set of k counting sections, one inside each isolating block, is called a *system of counting sections associated to \mathcal{V}* .

We are interested in trajectories that go inside a neighbourhood V_j in positive time and hit the counting section Π_j a finite number of times (which can be zero) until they leave the neighbourhood. Every time the trajectory makes a turn inside V_j it hits the counting section (see figure 1 (a)). Hence, it is natural to have the following definition where $\text{int}(A)$ is the interior of $A \subset M$:

Definition 1. *Let c_j be a periodic trajectory of saddle type, with V_j an isolating block for c_j and Π_j a counting section. Let $q \in \partial V_j$ be a point such that the following properties hold:*

- $\exists \tau > 0, \forall t \in (0, \tau), \varphi(t, q) \in \text{int}(V_j)$
- $\varphi(\tau, q) \in \partial V_j$.

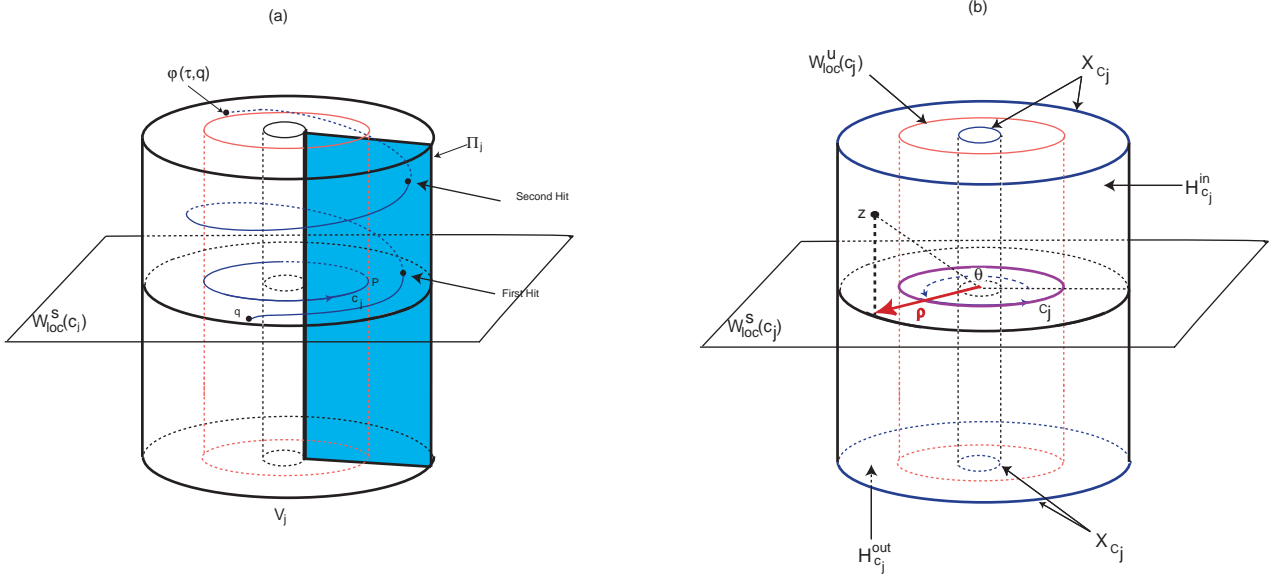


FIGURE 1. (a): Example of a trajectory turning twice around a periodic trajectory c_j , in V_j with respect to Π_j . (b): General cylindrical coordinates on the neighbourhood V_j of c_j and isolating blocks. The set $H_{c_j}^{in}$ is formed by two cylinder walls, the set $H_{c_j}^{out}$ corresponds to the top and bottom annuli and $X_{c_j} = \overline{H_{c_j}^{in}} \cap \overline{H_{c_j}^{out}}$ consists of four circles.

The trajectory of q turns n times around c_j in V_j , relatively to Π_j if

$$\#(\{\phi(t, q), t \in [0, \tau]\} \cap \Pi_j) = n \geq 0.$$

Definition 2. A heteroclinic cycle $\Sigma = \langle c_1, \dots, c_k \rangle$ of periodic trajectories has cycling if there exist:

- V_Σ a neighbourhood of Σ ;
- $\mathcal{V} = \{V_j\}_{j \in \{1, \dots, k\}}$ a system of isolating blocks;
- $\{\Pi_j\}_{j \in \{1, \dots, k\}}$ a system of counting sections;

such that given an index set I to be specified below, for any sequence of nonnegative integers $(z_i)_{i \in I}$, there exists a point q and there are times $(t_i^{in})_{i \in I}$ and $(t_i^{out})_{i \in I}$ satisfying $t_i^{in} < t_i^{out} < t_{i+1}^{in}$ such that, for each $i \in I$, if $i \equiv j \pmod{k}$:

- $\phi(t, q) \in V_\Sigma$ for $t \in [t_i^{in}, t_i^{out}]$ and for $t \in [t_i^{out}, t_{i+1}^{in}]$;
- for all $t \in (t_i^{in}, t_i^{out})$, the trajectory $\phi(t, q)$ lies in $\text{int}(V_j)$;
- for $t \in [t_i^{in}, t_i^{out}]$, the trajectory $\phi(t, q)$ turns z_i times around c_j , in V_j , with respect to Π_j ;
- for $t \in (t_i^{out}, t_{i+1}^{in})$, $\phi(t, q)$ does not visit the isolating block for any node in Σ .

When the property above holds for a finite index set $I = \{1, \dots, m\}$, then Σ has finite cycling of order m .

When it holds for $I = \mathbf{Z}$ then Σ has bi-infinite cycling (also called chaotic double cycling for reasons that will be apparent in the sequel).

We refer to the difference $t_j^{out} - t_j^{in}$ as the *time of flight* of the first visit of the trajectory $\phi(t, q)$ to V_j .

For a heteroclinic network Σ^* with node set $\mathcal{A} = \{c_j\}_{j=1, \dots, k}$, a *path on Σ^** is an infinite sequence (s_l) of connections $s_l = [x_l \rightarrow y_l]$ in Σ^* such that $x_l, y_l \in \mathcal{A}$ and $y_l = x_{l+1}$, thus forming a connected graph. For each heteroclinic connection in a network Σ^* , consider a point p on it and a small neighbourhood V of p , so that these neighbourhoods are pairwise disjoint. Given a system of isolating blocks for the nodes of Σ^* , if a trajectory $\varphi(t)$ visits all these neighbourhoods in the same sequence as the path (s_l) we say it *follows the path (s_l)* .

There is *switching near Σ^** if for each system of neighbourhoods as above and for each path on Σ^* there is a trajectory that follows it. See Aguiar *et al* [3, 5] for a detailed discussion of these concepts.

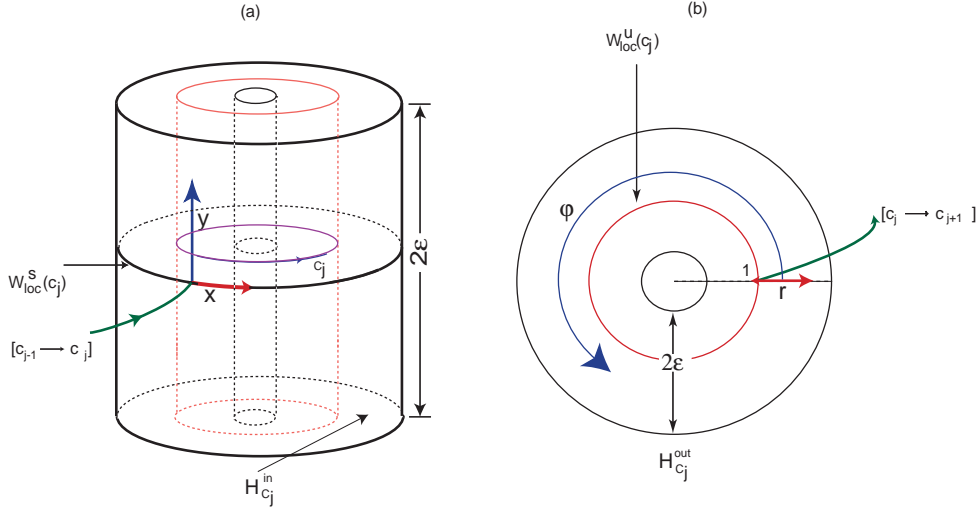


FIGURE 2. Isolating block for the closed trajectory c_j . (a): coordinates on the walls of the hollow cylinder (cross section *in*); (b): coordinates on the top and bottom of the hollow cylinder (cross section *out*). The flow enters the hollow cylinder transversely across the cylinder walls $H_{c_j}^{in}$ and leaves it transversely across the top and bottom $H_{c_j}^{out}$.

3. LOCAL DYNAMICS AND TRANSITION MAPS

In this section, we obtain a system of isolating blocks for a cycle $\Sigma = \langle c_1, \dots, c_k \rangle$ of periodic trajectories in a 3-dimensional manifold. We also establish the notation for the proof of our main results in 3 dimensions.

3.1. Suspension. Consider a local cross-section Π_j at a point p_j in c_j , for $j \in \{1, \dots, k\}$. Since c_j is hyperbolic, by a result of Hartman [18], there is a neighbourhood V_j^* of p_j in Π_j where the first return map π_j is C^1 conjugate to its linear part. The eigenvalues of $d\pi_j$ are e^{E_j} and e^{-C_j} , where $E_j > 0$ and $C_j > 0$.

Suspending the linear map gives rise, in cylindrical coordinates (ρ, θ, z) around c_j (see figure 1 (b)), to the system of differential equations:

$$(2) \quad \begin{cases} \dot{\rho} = -C_j(\rho - 1) \\ \dot{\theta} = 1 \\ \dot{z} = E_j z \end{cases}$$

which is equivalent to the original flow near c_j , although the suspension does not preserve the return time of the original trajectories. In these coordinates, the periodic trajectory c_j is the circle defined by $\rho = 1$ and $z = 0$, its local stable manifold, $W_{loc}^s(c_j)$, is the plane $z = 0$ and $W_{loc}^u(c_j)$ is the surface defined by $\rho = 1$.

3.2. Isolating blocks for c_j . We will work with a hollow three-dimensional cylindrical neighbourhood $V_j(\varepsilon)$ of c_j contained in the suspension of V_j^*

$$V_j(\varepsilon) = \{(\rho, \theta, z) : 1 - \varepsilon \leq \rho \leq 1 + \varepsilon, -\varepsilon \leq z \leq \varepsilon \text{ and } \theta \in \mathbf{R} \pmod{2\pi}\}.$$

When there is no ambiguity, we write V_j instead of $V_j(\varepsilon)$. Its boundary (see figure 1 (b)) is a disjoint union

$$\partial V_j = H_{c_j}^{in} \cup H_{c_j}^{out} \cup X_{c_j}$$

such that :

- $H_{c_j}^{in}$ is the union of the walls, $\rho = 1 \pm \varepsilon$, of the cylinder, locally separated by $W^u(c_j)$. Trajectories starting at $H_{c_j}^{in}$ go inside the cylinder V_j in small positive time.

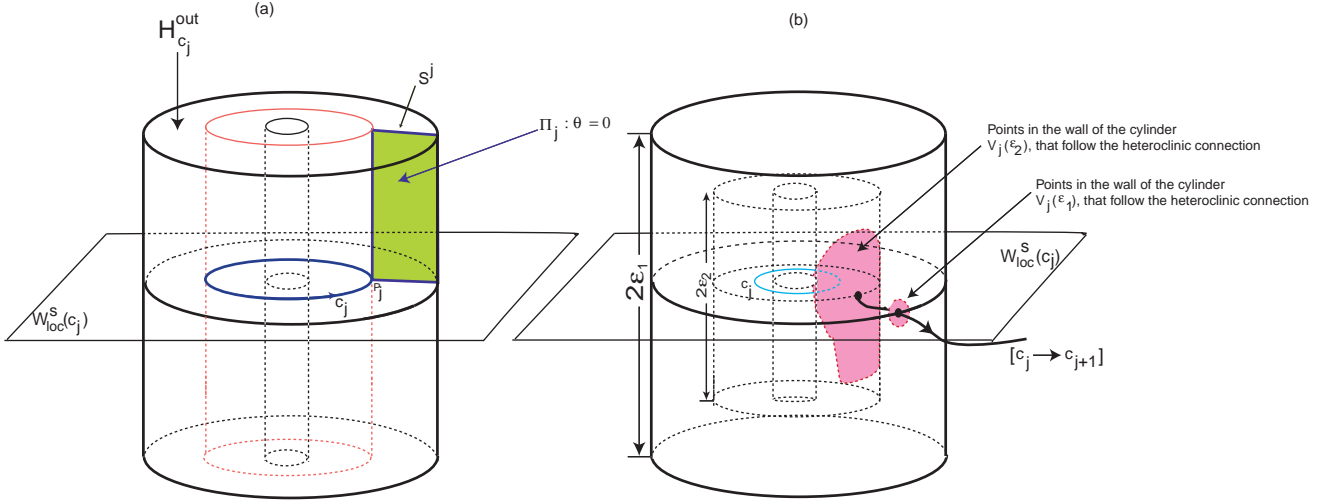


FIGURE 3. (a): The counting section Π_j at c_j is represented by the shaded rectangle and the segment S^j is $\Pi_j \cap H_{c_j}^{out}$; (b) Subsets where a flow-box around the connection $[c_j \rightarrow c_{j+1}]$ meets the boundary of cylindrical neighbourhoods $V_j(\varepsilon_2) \subset V_j(\varepsilon_1)$ of c_j . If $\varepsilon_1 > \varepsilon_2 > 0$ the intersection is a larger set, due to the expanding Floquet exponent at each node.

- $H_{c_j}^{out}$ is the union of two annuli, the top and the bottom, $z = \pm\varepsilon$ of the cylinder, locally separated by $W^s(c_j)$. Trajectories starting at $H_{c_j}^{out}$ go inside the cylinder V_j in small negative time.
- The vector field is transverse to ∂V_j at all points except at the four circles $X_{c_j} = \overline{H_{c_j}^{in}} \cap \overline{H_{c_j}^{out}}$.

The two cylinder walls, $H_{c_j}^{in}$ are parametrised by the covering maps:

$$(\theta_0, z_0) \mapsto (1 \pm \varepsilon, \theta_0, z_0) = (\rho, \theta, z),$$

where $\theta_0 \in \mathbf{R} \pmod{2\pi}$, $|z_0| < \varepsilon$ (see figure 2 (a)). In these coordinates, $H_{c_j}^{in} \cap W^s(c_j)$ is the union of the two circles $z_0 = 0$. The two annuli $H_{c_j}^{out}$ are parametrised by the coverings:

$$(\varphi, r) \mapsto (r, \varphi, \pm\varepsilon) = (\rho, \theta, z),$$

for $1 - \varepsilon < r < 1 + \varepsilon$ and $\varphi \in \mathbf{R} \pmod{2\pi}$ and where $H_{c_j}^{out} \cap W^u(c_j)$ is the union of the two circles $r = 1$ (see figure 2 (b)). In these coordinates $X_{c_j} = \overline{H_{c_j}^{in}} \cap \overline{H_{c_j}^{out}}$ is the union of the four circles defined by $\rho = 1 \pm \varepsilon$ and $z = \pm\varepsilon$.

3.3. Local map near c_j . For each $j \in \{1, \dots, k\}$, in the above coordinates, there are local maps ϕ_{c_j} from a connected component of $H_{c_j}^{in}$ into a connected component of $H_{c_j}^{out}$, given by:

$$(3) \quad \phi_{c_j}(\theta_0, z_0) = \left(\theta_0 - \frac{1}{E_j} \ln \left(\frac{z_0}{\varepsilon} \right), 1 \pm \varepsilon \left(\frac{z_0}{\varepsilon} \right)^{\delta_j} \right) = (\varphi, r) \quad \text{where} \quad \delta_j = \frac{C_j}{E_j} > 0.$$

The signs \pm depend on the component of $H_{c_j}^{in}$ we started at, $+$ for trajectories starting with $\rho > 1$ and $-$ for $\rho < 1$. From now on we use as counting section the rectangle, denoted by Π_j

$$\Pi_j = \{(\rho, \theta, z) : \theta = 0, \quad 1 \leq \rho \leq 1 + \varepsilon \quad \text{and} \quad 0 \leq z \leq \varepsilon\}.$$

We denote by S^j its intersection with $H_{c_j}^{out}$ (see figure 3 (a)). Without loss of generality we assume each connection $[c_j \rightarrow c_{j+1}]$ meets $H_{c_j}^{out}$ far from the counting section Π_j .

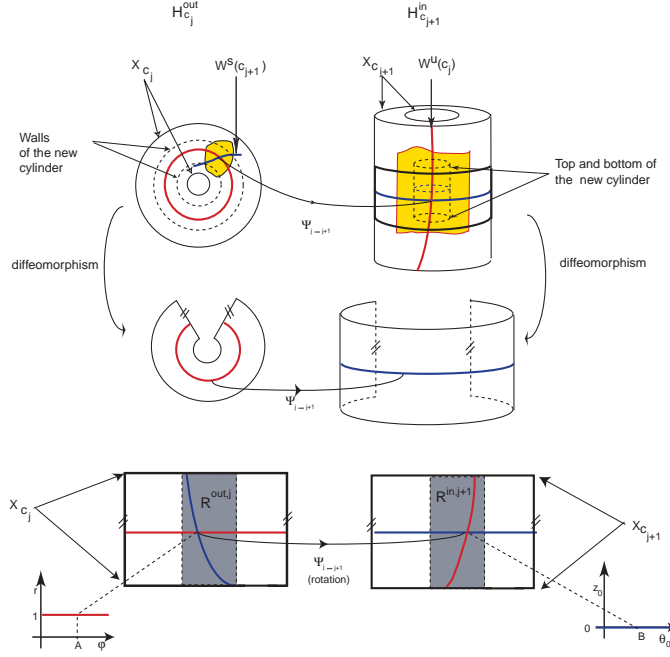


FIGURE 4. The transition map, defined near the connection $[c_j \rightarrow c_{j+1}]$, maps the invariant manifold $W^u(c_j)$ across $H_{c_{j+1}}^{in}$, if V_j and V_{j+1} are sufficiently small. By taking a smaller cylinder we obtain a rectangle $\mathcal{R}^{out,j}$ centered at $H_{c_j}^{out} \cap [c_j \rightarrow c_{j+1}]$ such that two opposite sides lie in X_{c_j} and $\Psi_{j \rightarrow j+1}(\mathcal{R}^{out,j}) \cap H_{c_{j+1}}^{in}$ is a rectangle with the same property in $H_{c_{j+1}}^{in}$.

3.4. Transition maps from c_j to c_{j+1} . Using the parametrisations above, let $(A, 1) = (\varphi, r)$ be the coordinates of the point in $[c_j \rightarrow c_{j+1}] \cap H_{c_j}^{out}$ and let $(B, 0) = (\theta_0, z_0)$ be the coordinates of $[c_j \rightarrow c_{j+1}] \cap H_{c_{j+1}}^{in}$, with $c_{k+1} = c_1$. A flow-box around a piece of $[c_j \rightarrow c_{j+1}]$ containing these two points meets $H_{c_j}^{out}$ and $H_{c_{j+1}}^{in}$ at neighbourhoods of $(A, 1)$ in $H_{c_j}^{out}$ and of $(B, 0)$ in $H_{c_{j+1}}^{in}$. A transition map $\Psi_{j \rightarrow j+1}$ is well defined in these neighbourhoods and C^1 close to a non trivial rotation (without loss of generality, for computations, we will use the rotation of $\frac{\pi}{2}$) (see figure 4).

The size of these neighbourhoods depend on the size, ε , of V_j and V_{j+1} ; for smaller values of ε , if we extend the flow-box the neighbourhood becomes larger due to the expanding Floquet exponent at each node as in figure 3 (b). Since $W^u(c_j)$ and $W^s(c_{j+1})$ meet transversely, we may take a sufficiently small ε for the neighbourhood V_j so the part of $W_{loc}^u(c_j)$ that lies inside the neighbourhood is mapped by $\Psi_{j \rightarrow j+1}$ across the height of $H_{c_{j+1}}^{in}$ as in figure 4. Thus it is possible to define a region $\mathcal{R}^{in,j+1}$ parametrised by a rectangle in $H_{c_{j+1}}^{in}$ around $(B, 0)$, contained in the image of $\Psi_{j \rightarrow j+1}$ and such that two opposite sides of $\mathcal{R}^{in,j+1}$ are contained in $X_{c_{j+1}}$. Moreover, $\mathcal{R}^{in,j+1}$ will contain the image of a piece of $\Psi_{j \rightarrow j+1}(W_{loc}^u(c_j))$ joining two components of X_{c_j} (see figure 4). We will call $\mathcal{R}^{in,j+1}$ a *rectangle in $H_{c_{j+1}}^{in}$* . Note that once this holds for V_j , the same is true for all hollow cylinder neighbourhoods of c_j with smaller size ε . Thus, we may also have a piece of $W_{loc}^s(c_{j+1})$ mapped by $\Psi_{j \rightarrow j+1}^{-1}$ across the width of $H_{c_j}^{out}$ and meeting X_{c_j} at two points, reducing ε if necessary.

It will also be convenient to assume that, for each j , $\mathcal{R}^{in,j}$ does not intersect S^j , the boundary of the section where turns are counted. This may be achieved by changing the position of the sections if necessary. For sections 4 and 5, we are always considering the system of isolating blocks $\mathcal{V} = \{V_j\}_j$ defined in this section and satisfying these properties.

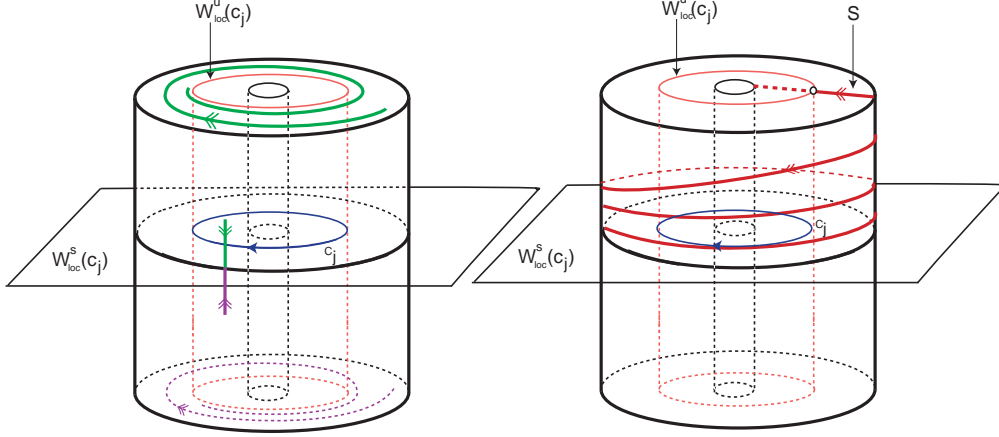


FIGURE 5. Local dynamics in the neighbourhood of the periodic solution c_j (see lemma 1). Left: any segment in $H_{c_j}^{in}$ is mapped into a helix in $H_{c_j}^{out}$ accumulating on $W_{loc}^u(c_j) \cap H_{c_j}^{out}$. Right: the image of any segment in $H_{c_j}^{out}$, by $\phi_{c_j}^{-1}$, a helix accumulating on $W_{loc}^s(c_j) \cap H_{c_j}^{in}$. The double arrow on the lines represents the orientation and not the flow.

4. GEOMETRY NEAR THE NODES

The notation and constructions of section 3 may now be used to study the geometry associated to the local dynamics around each node of the heteroclinic cycle Σ .

Definition 3. A segment β on $H_{c_j}^{in}$ is a smooth regular parametrized curve $\beta : [0, 1] \rightarrow H_{c_j}^{in}$, that meets $W_{loc}^s(c_j)$ transversely at the point $\beta(1)$ only and such that, writing $\beta(s) = (x(s), y(s))$, both x and y are monotonic functions of s . A restriction of any segment to an interval not containing 1, will be called a piece of segment.

Definition 4. Let $a, b \in \mathbf{R}$ such that $a < b$ and let H be a surface parametrized by a covering $(\theta, h) \in \mathbf{R} \times [a, b]$ where θ is periodic. A helix on H accumulating on the circle $h = h_0$ is a curve $\gamma : [0, 1) \rightarrow H$ such that its coordinates $(\theta(s), h(s))$ are monotonic functions of s with

$$\lim_{s \rightarrow 1^-} h(s) = h_0 \quad \text{and} \quad \lim_{s \rightarrow 1^-} |\theta(s)| = +\infty.$$

Lemma 1. The image of a segment in $H_{c_j}^{in}$ by ϕ_{c_j} is a helix accumulating on $W_{loc}^u(c_j) \cap H_{c_j}^{out}$. Similarly $\phi_{c_j}^{-1}$ maps a segment in $H_{c_j}^{out}$ into a helix accumulating on $W_{loc}^s(c_j) \cap H_{c_j}^{in}$ (see figure 5).

Proof. The proof is a direct calculation using the expression (3) for ϕ_{c_j} and

$$\phi_{c_j}^{-1}(0, r) = \left(-\frac{\ln(\varepsilon)}{\varepsilon E_j} \left[\frac{\varepsilon}{1-r} \right]^{\frac{1}{\delta_j}} ; \varepsilon \left[\frac{1-r}{\varepsilon} \right]^{\frac{1}{\delta_j}} \right) \quad r \in (1-\varepsilon, 1)$$

defined into the component of $H_{c_j}^{in}$ with $\rho = 1 - \varepsilon$. For $r \in (1, 1 + \varepsilon)$ a similar expression holds. A similar proof may be found in Aguiar *et al* [5] (section 6, proposition 3). \square

From the same calculations it follows that for a point $q \in H_{c_j}^{in} \setminus W_{loc}^s(c_j)$ the closer it is to $W_{loc}^s(c_j)$ the larger will be the number of loops inside V_j of its trajectory (see figure 7). We also get:

Corollary 2. The inverse image $\phi_{c_j}^{-1}(S^j \setminus W_{loc}^u(c_j))$ has two connected components lying on $H_{c_j}^{in}$ and each component is a helix accumulating on $W_{loc}^s(c_j) \cap H_{c_j}^{in}$.

The next step is to compute the number of loops of a trajectory inside V_j . This is done using the linearised equations (2) and noting that the trajectory of $q = (\theta_0, z_0) \in H_{c_j}^{in} \setminus W_{loc}^s(c_j)$ arrives at $H_{c_j}^{out}$

at time

$$\tau = \frac{1}{E_j} \ln \left(\frac{\varepsilon}{z_0} \right).$$

Denoting by $[a]$ the greater integer less than or equal to a , we have:

Proposition 3. *The number of turns made by the trajectory of a point $q = (\theta_0, z_0) \in H_{c_j}^{in} \setminus W_{loc}^s(c_j)$ inside V_j with respect to Π_j is given by:*

$$\left[\left[\left(\frac{1}{E_j} \ln \left(\frac{\varepsilon}{z_0} \right) + \theta_0 \right) / 2\pi \right] \right].$$

The calculations used for proposition 3 yield:

Corollary 4. *If β is a piece of segment meeting transversely $\phi_{c_j}^{-1}(S^j \setminus W^u(c_j))$ only at the end points, then $\phi_{c_j}(\beta)$ is a piece of helix on the annulus $H_{c_j}^{out}$ meeting S^j only at its end points.*

From corollary 4, it follows that:

Corollary 5. *If β is a piece of segment meeting $\phi_{c_j}^{-1}(S^j \setminus W^u(c_j))$ transversely with end points lying in $\phi_{c_j}^{-1}(S^j)$, then $\phi_{c_j}(\beta)$ is a piece of helix turning $m - 1$ times around $W^u(c_j) \cap H_{c_j}^{out}$ relatively to S^j on the annulus $H_{c_j}^{out}$, where m is the number of elements of the set $\phi_{c_j}^{-1}(S^j) \cap \beta$.*

5. CHAOTIC DOUBLE CYCLING IN 3-DIMENSIONS

In this section we put together all the information about the local maps to prove:

Theorem 6. *Let $\Sigma = \langle c_1, \dots, c_k \rangle$ be a heteroclinic cycle of hyperbolic periodic trajectories in a 3-dimensional manifold such that the invariant manifolds of consecutive nodes of Σ meet transversely. Then:*

- a) *in every neighbourhood of Σ there is a suspension of an invariant Cantor set of trajectories that follow Σ in positive and negative time;*
- b) *Σ has bi-infinite cycling.*

The proof of theorem 6 uses symbolic dynamics and occupies all of this section. We define a discretisation of the flow and then the result follows from standard methods in symbolic dynamics, see for instance Kitchens [23] and Wiggins [43, 44]. The only delicate point is the construction of the non-wandering set of statement a) where the discretised flow may be indefinitely iterated. In 5.2 and 5.3 we construct the intersection of the non-wandering set with $H_{c_j}^{in}$ and $H_{c_j}^{out}$ and then in 5.4 we move it to the counting sections Π_j . This is the part of the proof for which we have to modify the methods of Wiggins [44], the rest follows from the same arguments given in that source. Then in section 6 we look at extensions and consequences, both of theorem 6 and of the method used for the proof. We start with some terminology.

5.1. Strips. Given a region \mathcal{R} in $H_{c_j}^{in}$ or in $H_{c_j}^{out}$ parametrized by a rectangle $R = [w_1, w_2] \times [z_1, z_2]$, a *horizontal strip* in \mathcal{R} will be parametrized by:

$$\mathcal{H} = \{(x, y) : x \in [w_1, w_2], y \in [u_1(x), u_2(x)]\},$$

where

$$u_1, u_2 : [w_1, w_2] \rightarrow [z_1, z_2]$$

are Lipschitz functions such that $u_1(x) < u_2(x)$.

The *horizontal boundaries* of the strip are the lines parametrized by the graphs of the u_i , the *vertical boundaries* are the lines $\{w_i\} \times [u_1(w_i), u_2(w_i)]$ and its *height* is

$$h = \max_{x \in [w_1, w_2]} (u_2(x) - u_1(x)).$$

When both $u_1(x)$ and $u_2(x)$ are constant functions we call \mathcal{H} a *horizontal rectangle across \mathcal{R}* .

A *vertical strip across \mathcal{R}* , its *width* and a *vertical rectangle* have similar definitions, with the roles of x and y reversed. A *strip* in $H_{c_j}^{in}$ is the intersection of a vertical strip and a horizontal strip. From corollary 4, it follows:

Corollary 7. *If \mathcal{S} is a strip in $H_{c_j}^{in}$ such that:*

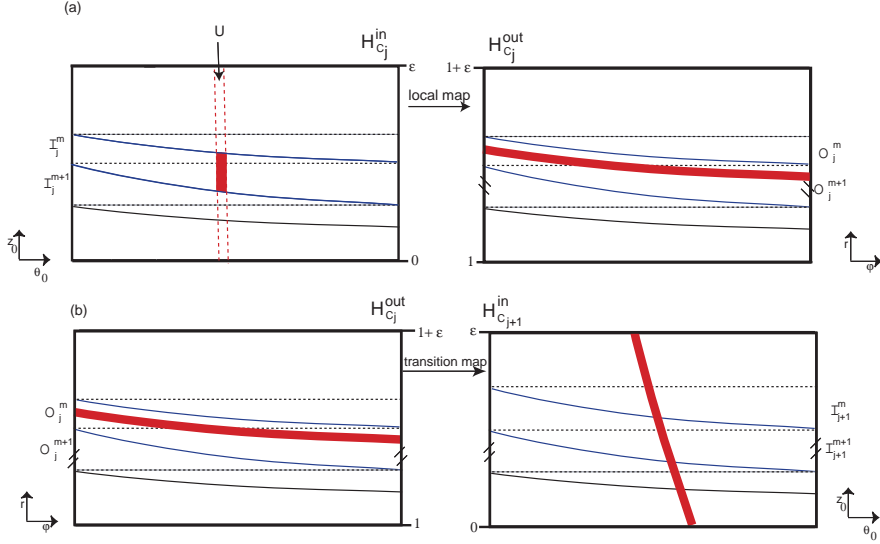


FIGURE 6. (a): If a strip in the cylinder $H_{c_j}^{in}$ has its horizontal boundaries in $\phi_{c_j}^{-1}(S^j)$ then its image by ϕ_{c_j} makes a complete turn in the annulus $W_{loc}^u(c_j) \cap H_{c_j}^{out}$ (corollary 7). (b): The image by $\Psi_{j \rightarrow j+1}$ of a horizontal strip in $H_{c_j}^{out}$ is a vertical strip in $H_{c_{j+1}}^{in}$.

- the horizontal boundaries of \mathcal{S} lie in $\phi_{c_j}^{-1}(S^j)$
- $\text{int}(\mathcal{S}) \cap \phi_{c_j}^{-1}(S^j) = \emptyset$,

then ϕ_{c_j} maps \mathcal{S} into a horizontal strip in $H_{c_j}^{out}$ having two intervals in S^j as vertical boundaries and whose horizontal boundaries consist of two arcs of helices, each one starting and ending at S^j , that make a complete turn around $W_{loc}^u(c_j) \cap H_{c_j}^{out}$ (see figure 6 (a)).

5.2. Partitions. For the proof of theorem 6, consider a small neighbourhood of Σ , with a system of isolating blocks $\mathcal{V} = \{V_j\}_{j \in \{1, \dots, k\}}$ and counting sections $\{\Pi_j\}_{j \in \{1, \dots, k\}}$ associated to \mathcal{V} as defined in section 3. We restrict our attention to the rectangles, constructed in 3.4, where the transition maps are well defined and to the $z \geq 0$ and $\rho \geq 1$ components of $H_{c_j}^{in}$ and $H_{c_j}^{out}$, that we continue to represent by the same symbols.

The set $\overline{H_{c_j}^{in}} \setminus W_{loc}^s(c_j)$ is partitioned into subsets \mathcal{I}_j^m of points whose trajectory hits m times the counting section Π_j without leaving V_j (figure 7). A partition of $\overline{H_{c_j}^{out}} \setminus W_{loc}^u(c_j)$ into sets \mathcal{O}_j^m , $m \in \mathbf{N}$, is defined in a similar way.

For $m \in \mathbf{N}$ the closure $\overline{\mathcal{I}_j^m}$ is a horizontal strip in $H_{c_j}^{in}$ and it also intersects in a horizontal strip the rectangle $\mathcal{R}^{in,j}$ where the transition map $\Psi_{j-1 \rightarrow j}$ is well defined. The elements \mathcal{I}_j^m of the partition are connected sets with vertical boundary consisting of two pieces of $\partial\Pi_j$ and horizontal boundary consisting of two arcs of $\phi_{c_j}^{-1}(S^j \setminus W_{loc}^u(c_j)) = \phi_{c_j}^{-1}([\partial\Pi_j \cap H_{c_j}^{out}] \setminus W_{loc}^u(c_j))$ (figures 6 (a) and 7).

Let U be a vertical strip across $\mathcal{R}^{in,j}$. The following properties follow from the results of sections 3 and 4 and from corollary 7:

- (1) By corollary 7, for $m \in \mathbf{N}$ the set $\widehat{U} = \phi_{c_j}(U \cap \overline{\mathcal{I}_j^m})$ is a horizontal strip across the width of $H_{c_j}^{out}$ (figure 6 (a)) and thus $\widehat{U} \cap \mathcal{R}^{out,j}$ is a horizontal strip;
- (2) If the vertical boundaries of U are the graphs of smooth monotonically decreasing functions, then the horizontal boundaries of $\widehat{U} \cap \mathcal{R}^{out,j}$ are the graphs of smooth monotonically decreasing functions;
- (3) The set $\widetilde{U} = \Psi_{j \rightarrow j+1}(\widehat{U} \cap \mathcal{R}^{out,j})$ is a vertical strip across $\mathcal{R}^{in,j+1} \subset H_{c_{j+1}}^{in}$ (figure 6 (b)).

Going backwards in time we get dual results, for U a horizontal strip across $\mathcal{R}^{in,j}$:

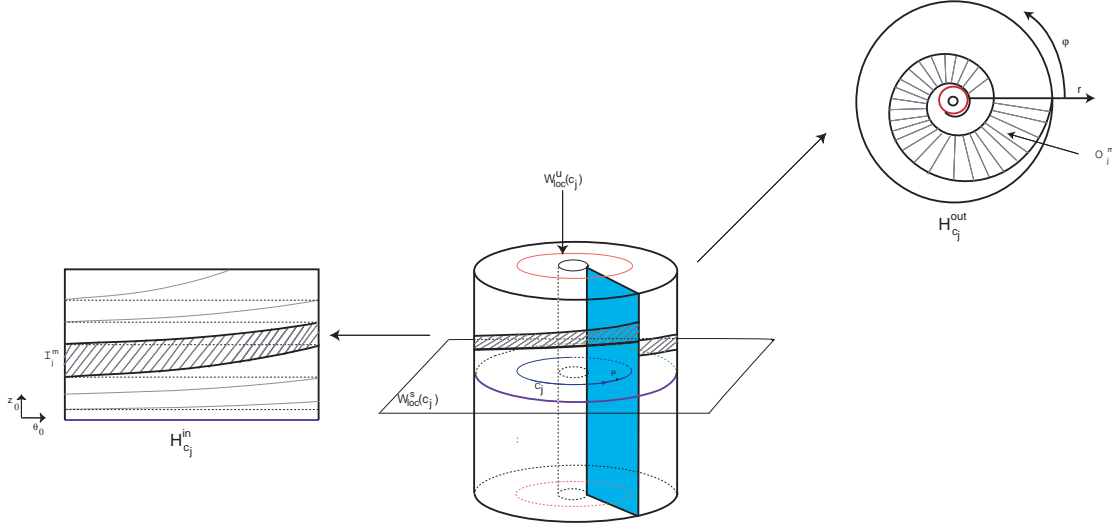


FIGURE 7. Partitions of $H_{c_j}^{in}$ and $H_{c_j}^{out}$ corresponding to trajectories that make any integer number of turns in V_j . For a point $q \in H_{c_j}^{in} \setminus W_{loc}^s(c_j)$ the closer it is to $W_{loc}^s(c_j)$ the larger will be the number of loops inside V_j of its trajectory.

- (4) The set $\Psi_{(j-1) \rightarrow j}^{-1}(U)$ is a vertical strip across $\mathcal{R}^{out,j-1} \subset H_{c_{j-1}}^{out}$.

We get dual results, for W a vertical strip across $\mathcal{R}^{out,j-1}$:

- (5) For $m \in \mathbf{N}$, the set $\widehat{W} = W \cap \overline{\mathcal{O}_{j-1}^m}$ is a strip in $H_{c_{j-1}}^{out}$ with horizontal boundaries contained in $S^{i,j} = \phi_{c_{j-1}}(\Pi_{j-1} \cap H_{c_{j-1}}^{in})$;
- (6) The set $\phi_{c_{j-1}}^{-1}(\widehat{W})$ is a horizontal strip across $\mathcal{R}^{in,j-1} \subset H_{c_{j-1}}^{in}$ (by the dual of corollary 7);
- (7) If the vertical boundaries of W are the graphs of smooth monotonically increasing functions, then the horizontal boundaries of $\phi_{c_{j-1}}^{-1}(\widehat{W}) \cap \mathcal{R}^{in,j-1}$ are the graphs of smooth monotonically increasing functions;
- (8) The set $\widetilde{W} = \Psi_{(j-2) \rightarrow (j-1)}^{-1}(\phi_{c_{j-1}}^{-1}(\widehat{W}) \cap \mathcal{R}^{in,j-1})$ is a vertical strip across $\mathcal{R}^{out,j-2}$.

5.3. First coding. We start by the description of the set of points whose trajectory makes a prescribed number of turns around each node in Σ , the phenomenon that we call cycling. From now on we assume the indexing over the k symbols for the nodes is always done (mod k).

Since we are assuming that the invariant manifolds $W^u(c_j)$ and $W^s(c_{j+1})$ meet transversely, then $W_{loc}^s(c_{j+1}) \cap H_{c_j}^{out}$ is the graph of a smooth function $(\varphi(r), r)$. From transversality it follows that the function $\varphi(r)$ is monotonic near $r = 1$ for $r - 1 > 0$ small. In what follows, for the sake of definiteness, we will assume that this function is either decreasing or constant. If it is an increasing function the main result still holds, but either we would have to change the choice of parametrisation or we would have to adapt the intermediate statements. Similarly, without loss of generality, the curve $(\theta_0(z_0), z_0)$ representing $W_{loc}^u(c_j) \cap H_{c_{j+1}}^{in}$ is assumed to be the graph of a monotonically decreasing function for $z_0 > 0$ near $z_0 = 0$.

Given a natural number m and a subset U of $\mathcal{R}^{in,j}$ consider the set $P_j(m, U)$ given by:

$$P_j(m, U) = \Psi_{j \rightarrow (j+1)}(\phi_{c_j}(U \cap \overline{\mathcal{I}_j^m}) \cap \mathcal{R}^{out,j}) \subset \mathcal{R}^{in,j+1} \subset H_{c_{j+1}}^{in}.$$

From properties (1) - (3) and a direct calculation, it follows that if U is a vertical strip across $\mathcal{R}^{in,j}$ then:

- (9) the set $P_j(m, U)$ is a vertical strip across $\mathcal{R}^{in,j+1}$;
- (10) If the vertical boundaries of U are the graphs of smooth monotonically decreasing functions then the vertical boundaries of $P_j(m, U)$ are the graphs of smooth monotonically decreasing functions;

- (11) If moreover the width of U is d then the width of $P_j(m, U)$ is at most $\mu_m d$ for $\mu_m = \varepsilon C_j e^{-2\pi C_j(m-1)}$. Note that $\mu_m < 1$ for all $m > 0$ if $\varepsilon < 1/C_j$ (see lemma 18 in appendix A).

Note that if U is a vertical strip across $\mathcal{R}^{in,j}$, then $P_j(m, U)$ is the image by $\Psi_{j \rightarrow (j+1)}$ of a horizontal strip across $H_{c_j}^{out}$ and it is transformed into a vertical strip across $H_{c_{j+1}}^{in}$ intersecting \mathcal{I}_{j+1}^m , for all m . Here we are using the property of the neighbourhoods V_j we have constructed in 3.4.

Similarly, to each natural number m and each subset W of $\mathcal{R}^{out,j}$ we associate a subset $Q_j(m, W)$ of $\mathcal{R}^{out,j-1}$ given by

$$Q_j(m, W) = \Psi_{(j-1) \rightarrow j}^{-1} \left(\phi_{c_j}^{-1} (W \cap \overline{\mathcal{O}_j^m}) \cap \mathcal{R}^{in,j} \right) \subset \mathcal{R}^{out,j-1} \subset H_{c_{j-1}}^{out}.$$

If W is a vertical strip across $\mathcal{R}^{out,j}$ then from properties (4) - (8) we get:

- (12) The set $Q_j(m, W)$ is a vertical strip across $\mathcal{R}^{out,j-1}$;
(13) If the vertical boundaries of W are the graphs of smooth monotonically decreasing functions then the vertical boundaries of $Q_j(m, W)$ are the graphs of smooth monotonically decreasing functions;
(14) If moreover the width of W is d then the width of $Q_j(m, U)$ is at most $\nu_m d$ for $\nu_m = \varepsilon E_j e^{-2\pi E_j m}$. Note that $\nu_m < 1$ for all $m \geq 0$ if $\varepsilon < 1/E_j$ (see lemma 18 in appendix A).

For $j = 1, \dots, k$, denote by Φ_j the expression

$$\Phi_j = \phi_{c_j} \circ \Psi_{(j-1) \rightarrow j} : \mathcal{R}^{out,j-1} \rightarrow \mathcal{R}^{out,j}.$$

Points q in $\mathcal{R}^{out,j}$ whose forward trajectory follows the cycle from c_j to c_{j+1} and arrive at $\Phi_{j+1}(q) \in \mathcal{R}^{out,j+1}$ lie in the set

$$W_j^1 = \bigcup_{m=1}^{\infty} Q_{j+1}(m, \mathcal{R}^{out,j+1}) \subset \mathcal{R}^{out,j}$$

which is the disjoint union of vertical strips across $\mathcal{R}^{out,j}$. Points q in $\mathcal{R}^{out,j}$ with forward trajectories that follow the connections $[c_j \rightarrow c_{j+1}]$ and $[c_{j+1} \rightarrow c_{j+2}]$ to arrive at $\Phi_{j+2} \circ \Phi_{j+1}(q) \in \mathcal{R}^{out,j+2}$ lie in the set

$$W_j^2 = \bigcup_{m=1}^{\infty} Q_{j+1}(m, W_{j+1}^1) \subset W_j^1 \subset \mathcal{R}^{out,j},$$

a disjoint union of vertical strips. Similarly points q with forward trajectory that follows the cycle along l connections from c_j to c_{j+l} , arriving at $\Phi_{j+l} \circ \dots \circ \Phi_{j+1}(q) \in \mathcal{R}^{out,j+l}$ lie in the set $W_j^l \subset \mathcal{R}^{out,j}$ defined recursively by

$$W_j^0 = \mathcal{R}^{out,j} \quad W_j^l = \bigcup_{m=1}^{\infty} Q_{j+1}(m, W_{j+1}^{l-1}) \subset W_j^{l-1} \subset \mathcal{R}^{out,j}$$

a disjoint union of vertical strips across $\mathcal{R}^{out,j}$, the *vertical strips in W_j^l* . We obtain chains of nested strips comprising the sets

$$\dots \subset W_j^{l+1} \subset W_j^l \subset W_j^{l-1} \subset \dots \subset W_j^1 \subset W_j^0.$$

The same procedure may be used going backwards in time. For $j = 1, \dots, k$, let

$$U_j^0 = \mathcal{R}^{in,j} \quad U_j^l = \bigcup_{m=1}^{\infty} P_{j-1}(m, U_{j-1}^{l-1}) \subset U_j^{l-1} \subset \mathcal{R}^{in,j},$$

where each U_j^l is a disjoint union of vertical strips across $\mathcal{R}^{in,j}$, the *vertical strips in U_j^l* . A point $q \in U_j^1$ lies in the forward trajectory of $p = \phi_{c_{j-1}}^{-1} \circ \Psi_{(j-1) \rightarrow j}^{-1}(q)$ that follows the connection $[c_{j-1} \rightarrow c_j]$ from $p \in \mathcal{R}^{in,j-1}$ to $q \in \mathcal{R}^{in,j}$. Let $\tilde{\Phi}_j^{-1}$ be given by $\tilde{\Phi}_j^{-1} = \phi_{c_j}^{-1} \circ \Psi_{j \rightarrow (j+1)}^{-1}$. Then the trajectory of a point $q \in U_j^l$, starting at $p = \tilde{\Phi}_{j-l}^{-1} \circ \dots \circ \tilde{\Phi}_{j-1}^{-1}(q) \in \mathcal{R}^{in,j-l}$ follows the l connections from c_{j-l} to c_j until it reaches q in $\mathcal{R}^{in,j}$.

The following properties of the sets U_j^l and W_j^l follow from direct calculations and from the properties (1)–(8) of section 5.2:

- (15) Each one of the vertical strips in W_j^l and in U_j^l , respectively, except for its horizontal boundaries is contained in the interior of a vertical strip, respectively in W_j^{l-1} and in U_j^{l-1} ;
- (16) The vertical boundaries of the strips in W_j^l and U_j^l are the graphs of smooth monotonically decreasing functions;
- (17) The first hit map Φ_{j+1} sends W_j^l onto W_{j+1}^{l-1} contracting the width of strips by $\nu < 1$, by construction;
- (18) The last hit map $\tilde{\Phi}_j^{-1}$ sends U_{j+1}^l onto U_j^{l-1} contracting the width of strips by $\mu < 1$, by construction;
- (19) The sets

$$\Lambda_j^{out} = \bigcap_{l=1}^{\infty} W_j^l \subset \mathcal{R}^{out,j} \quad \text{and} \quad \Lambda_j^{in} = \bigcap_{l=1}^{\infty} U_j^l \subset \mathcal{R}^{in,j}$$

are the disjoint union of graphs of smooth monotonically decreasing functions, the *curves in* Λ_j^{out} and Λ_j^{in} , respectively.

The trajectory of each point in one of the curves in Λ_j^{out} follows the cycle Σ for positive time t making the same number of turns around each node. The same holds in negative time t for the curves in Λ_j^{in} .

Each one of the sets Λ_j^{out} and Λ_j^{in} meets each horizontal line in $\mathcal{R}^{out,j}$ and $\mathcal{R}^{in,j}$, respectively, in an uncountable set of points. This intersection is not a Cantor set because it is not closed, since

$$\bigcup_{m=0}^{\infty} \overline{\mathcal{O}_j^m} = \overline{H_{c_j}^{out}} \setminus W_{loc}^u(c_j)$$

is not a closed set and for each l the strips in W_j^l accumulate on the vertical axis $W_{loc}^u(c_j) \cap \overline{H_{c_j}^{out}}$ but $W_{loc}^u(c_j) \cap W_j^l = \emptyset$, with a similar statement for U_j^l .

- (20) The set $\Psi_{(j-1) \rightarrow j}(\Lambda_{j-1}^{out}) \subset \mathcal{R}^{in,j}$ is the disjoint union of horizontal curves that are the graphs of smooth monotonic functions. Therefore, each vertical curve in Λ_j^{in} meets each horizontal curve in $\Psi_{(j-1) \rightarrow j}(\Lambda_{j-1}^{out})$ at exactly one point.

Let

$$\Lambda_j = \Lambda_j^{in} \cap \Psi_{(j-1) \rightarrow j}(\Lambda_{j-1}^{out}) \subset \mathcal{R}^{in,j} \quad \Lambda_{\mathbf{N}} = \bigcup_{j=1}^k \Lambda_j$$

and let $F : \Lambda_{\mathbf{N}} \rightarrow \Lambda_{\mathbf{N}}$ be given by $F(p) = \Psi_{j \rightarrow j+1} \circ \phi_{c_j}(p)$ for $p \in \mathcal{R}^{in,j}$. Then F may be indefinitely iterated in $\Lambda_{\mathbf{N}}$, so it defines a discrete dynamical system in $\Lambda_{\mathbf{N}}$. This proves statement a) of theorem 6. Moreover, for each point $p \in \Lambda_{\mathbf{N}}$ and each $l \in \mathbf{Z}$, if $p \in \Lambda_j$ then the point $F^l(p)$ lies in one of the strips \mathcal{I}_{j+l}^m in $\mathcal{R}^{in,j+l}$ so its trajectory turns m times around c_{j+l} . Thus to each point $p \in \Lambda_j$ and each $l \in \mathbf{Z}$ we associate $z_l(p) = m$.

The description of the number of turns made by trajectories of points in $\Lambda_{\mathbf{N}}$ may be rewritten in terms of symbolic dynamics, as follows. Let $\Omega_{\mathbf{N}} = \mathbf{N}^{\mathbf{Z}}$ be the space of bi-infinite sequences of natural numbers. We use for our first coding the space $\Omega_k = \{1, \dots, k\} \times \Omega_{\mathbf{N}}$, a non-compact metric space and the operator $\sigma_*(j, (z_i)) = (j+1, (z_{i+1}))$ on Ω_k , that is essentially the shift operator on $\Omega_{\mathbf{N}}$. For the topology of these spaces and the dynamics of σ see, for instance Kitchens[23], specially [23, Ch. 7] for shifts on infinite sets of symbols. Each symbol $(j, (z_i)) \in \Omega_k$ codes the number of turns z_i made by a trajectory around the node c_{i+j} as it follows the cycle $\Sigma = \langle c_1, \dots, c_k \rangle$. This is similar to the usual coding in symbolic dynamics, except that we are coding for number of turns instead of spatial dynamics and that we are keeping track of the node around which the turns are made.

Theorem 8. *The dynamical system $(\Lambda_{\mathbf{N}}, F)$ is topologically conjugate to the shift (σ_*, Ω_k) .*

This is why we call the dynamics a *horseshoe in time*: the number of turns in a neighbourhood of each closed orbit in the cycle, and consequently the time spent near each closed orbit, is coded like a horseshoe. Theorem 6 follows immediately from theorem 8.

5.4. Second coding. There are two problems with the coding of section 5.3. The first is that the set $\Lambda_{\mathbf{N}}$ of points in trajectories being coded is not closed, as we have already remarked. The second is that the corresponding symbolic dynamics uses an infinite set of symbols, and this has properties that are weaker than those of subshifts of finite type. We may overcome these difficulties by coding the trajectories of points in the counting sections Π_j , instead of taking points in $H_{c_j}^{in}$. The geometrical behaviour of the first return to Π_j is a lot more complicated than in $H_{c_j}^{in}$. For the sake of clarity we have used the first and simpler coding in $H_{c_j}^{in}$ and now we transfer the results to the counting sections, thus obtaining additional dynamical information that will be discussed in the next section.

Each counting section Π_j has been identified with the rectangle $(\rho, z) \in [1, 1 + \varepsilon] \times [0, \varepsilon]$ (see figures 3 (a) and 8 (a)). Then for each Π_j we consider a partition into horizontal rectangles (figure 8 (b)):

$$\mathcal{F}_j^m = [1, 1 + \varepsilon] \times (\varepsilon(e^{-2\pi E_j})^{m+1}, \varepsilon(e^{-2\pi E_j})^m) \quad m = 0, 1, \dots$$

and

$$\mathcal{F}_j^\infty = [1, 1 + \varepsilon] \times \{0\} = W^s(c_j) \cap \Pi_j$$

as well as a partition into vertical rectangles

$$\mathcal{G}_j^m = (1 + \varepsilon(e^{-2\pi C_j})^{m+1}, 1 + \varepsilon(e^{-2\pi C_j})^m) \times [0, \varepsilon] \quad m = 0, 1, \dots$$

and

$$\mathcal{G}_j^\infty = \{1\} \times [0, \varepsilon] = W^u(c_j) \cap \Pi_j .$$

Trajectories starting in $\Pi_j \setminus \mathcal{F}_j^0$ return to Π_j without leaving V_j , so there are well defined first hit maps $h_j : \Pi_j \setminus \mathcal{F}_j^0 \rightarrow \Pi_j$ that send each rectangle \mathcal{F}_j^m , $m \geq 1$ onto

$$h_j(\mathcal{F}_j^m) = \mathcal{F}_j^{m-1} \setminus \mathcal{G}_j^0 .$$

Their inverses h_j^{-1} are well defined in $\Pi_j \setminus \mathcal{G}_j^0$ and send each rectangle \mathcal{G}_j^m , $m \geq 1$ onto

$$h_j^{-1}(\mathcal{G}_j^m) = \mathcal{G}_j^{m-1} \setminus \mathcal{F}_j^0 .$$

Trajectories $\phi(t, q)$ starting at $q \in \mathcal{F}_j^0$ go out of V_j for positive t through H_j^{out} without crossing Π_j , so there are well defined first hit maps $f_j : \mathcal{F}_j^0 \rightarrow H_j^{out}$. Then, by (19) of section 5.3, the set $M_j^0 = f_j^{-1}(\Lambda_j^{out})$ is the disjoint union of horizontal curves across \mathcal{F}_j^0 that are the graphs of smooth monotonic functions.

Similarly, trajectories $\phi(t, q)$ of points $q \in \mathcal{G}_j^0$ come from outside V_j through H_j^{in} without crossing Π_j for negative t , so there are well defined last hit maps $g_j^{-1} : \mathcal{G}_j^0 \rightarrow H_j^{in}$ and $L_j^0 = g_j(\Lambda_j^{in})$ is the disjoint union vertical curves across \mathcal{G}_j^0 that are the graphs of smooth monotonic functions.

The maps h_j may now be used to obtain the first return to Π_j of trajectories of points in L_j^0 that do not go out of V_j without returning to Π_j . This is given by the set $L_j^1 = h_j(g_j(\Lambda_j^{in}) \setminus \mathcal{F}_j^0)$, a disjoint union vertical curves across \mathcal{G}_j^1 . Iterating the process we get $L_j^m = h_j(L_j^{m-1} \setminus \mathcal{F}_j^{m-1})$, a disjoint union vertical curves across \mathcal{G}_j^m . Similarly, define $M_j^m = h_j^{-1}(M_j^{m-1} \setminus \mathcal{G}_j^{m-1})$, a disjoint union of horizontal curves across \mathcal{F}_j^m .

The Cantor set

$$\Lambda = \bigcup_{j=1}^k \left(\mathcal{F}_j^\infty \cup \bigcup_{m=0}^{\infty} M_j^m \right) \cap \left(\mathcal{G}_j^\infty \cup \bigcup_{m=0}^{\infty} L_j^m \right) \subset \bigcup_{j=1}^k \Pi_j$$

consists of points whose trajectories return to $\bigcup_{j=1}^k \Pi_j$ infinitely many times in the future and in the past. The first return of $p \in \Lambda$ to $\bigcup_{j=1}^k \Pi_j$ is given by the map $G : \Lambda \rightarrow \Lambda$

$$G(p) = \begin{cases} h_j(p) & \text{for } p \in \Pi_j \setminus \mathcal{F}_j^0 \\ g_{j+1} \circ \Psi_{j \rightarrow (j+1)} \circ f_j(p) & \text{for } p \in \mathcal{F}_j^0 \end{cases}$$

and G may be indefinitely iterated in Λ . The expression for $G(p)$ is a well defined map in all of $\Pi_j \setminus \mathcal{F}_j^0$ and also in a vertical strip in \mathcal{F}_j^0 , but it has a discontinuity at the common boundary of \mathcal{F}_j^0 and \mathcal{F}_j^1 , if we use the induced topology in $\bigcup_j \Pi_j$.

Let $\Omega_T \subset \{1, \dots, k\}^{\mathbf{Z}}$ be the subspace of bi-infinite sequences of k symbols with transition matrix $T = (T_{ij})$ where $T_{ij} = 1$ if either $j = i$ or $j = i + 1 \pmod{k}$, $T_{ij} = 0$ otherwise and let σ be the shift

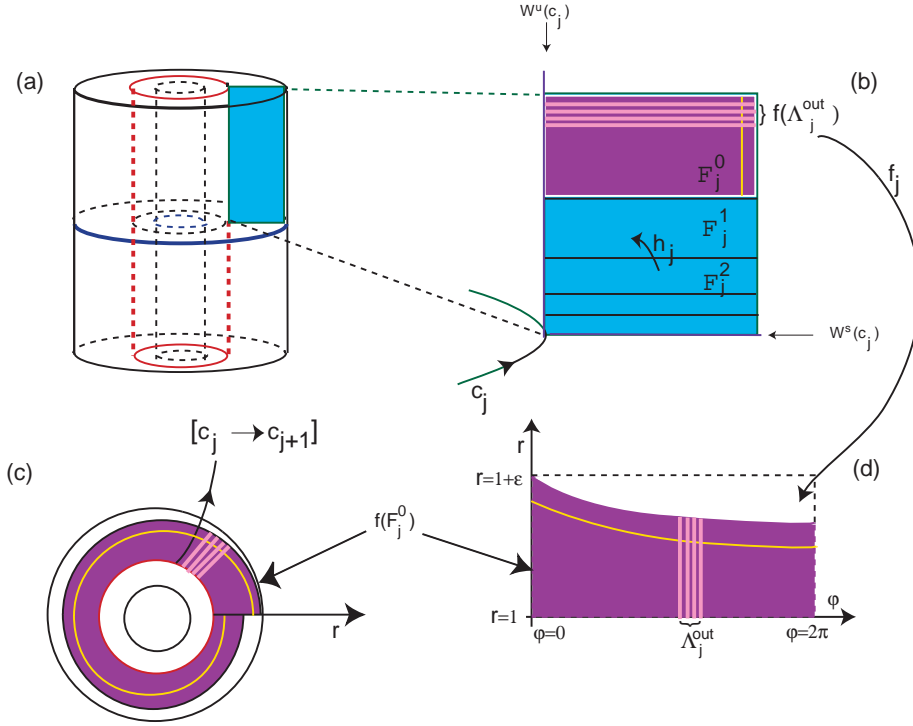


FIGURE 8. (a): The shaded rectangle represents the counting section Π_j at c_j . (b): The section Π_j may be partitioned into horizontal strips \mathcal{F}_j^m ($m \in \mathbf{N}_0$). For $m \geq 1$, the forward trajectory of a point in \mathcal{F}_j^m first hits Π_j at \mathcal{F}_j^{m-1} and then at \mathcal{F}_j^{m-2} and so on, until it reaches in \mathcal{F}_j^0 . The images of these points are governed by the map h_j . (c): The forward trajectory of a point in \mathcal{F}_j^0 goes to H_j^{out} without crossing Π_j . The shaded regions in (c) and (d) correspond to $h_j(\mathcal{F}_j^0)$. In (b), it is possible to see the representation of the Cantor set $f_j^{-1}(\Lambda_j^{out})$ as a disjoint union of horizontal strips across \mathcal{F}_j^0 . A similar statement holds for $g_j(\Lambda_j^{in})$ replacing horizontal strips across \mathcal{F}_j^0 by vertical strips across \mathcal{G}_j^0 .

operator on Ω_T . Given $p \in \Lambda$ and $i \in \mathbf{Z}$ let $s_i(p) = j$ if $G^i(p) \in \Pi_j$. This is a bijection from Λ onto Ω_T , by construction. The standard treatment of Wiggins [44] can now be used to yield:

Theorem 9. *The dynamical system (Λ, G) is topologically conjugate to (Ω_T, σ) .*

A sequence $(z_i)_{i \in \mathbf{Z}} \in \Omega_T$ gives us information about the number of turns around consecutive nodes of Σ of trajectories that remain close the cycle in forward and backward time. For example, if $k = 3$, the sequence

$$\dots 2233112233.1123333112233112233\dots$$

corresponds to a trajectory turning twice around c_1 , once around c_2 , four times around c_3 , twice around c_1 and so on. Each repetition of the symbol j corresponds to a new turn around c_j . Thus Theorem 6 follows from Theorem 9. Other interesting dynamical features are discussed in the next section.

6. EXTENSIONS AND DISCUSSION OF RESULTS

In this section we describe further consequences of the methods of Section 5 for the dynamics around the heteroclinic cycle Σ . The results are not the main goal of the paper, so the presentation is less detailed. From the results used theorem 8 it follows:

Corollary 10. *Let $\Sigma = \langle c_1, \dots, c_k \rangle$ be a heteroclinic cycle of hyperbolic periodic trajectories in a 3-dimensional manifold embedded in \mathbf{R}^n such that the invariant manifolds of consecutive nodes of Σ meet*

transversely. Then there exists a set with positive Lebesgue measure exhibiting finite cycling of any order and the finite cycling near Σ may be realized by periodic trajectories.

Proof. For this proof we use the first coding of section 5.3. Arbitrarily close to the cycle it is possible to define the set $\Lambda_{\mathbf{N}}$ as in Theorem 8. This set is constructed as an infinite intersection of nested strips U_j^l and $\Psi_{(j-1) \rightarrow j}(W_j^l)$. Each finite intersection of strips has positive measure in $\mathcal{R}^{in,j}$. Then for any m , points in the set

$$\bigcup_{j=1}^k \left(\bigcap_{l=1}^m U_j^l \cap \Psi_{(j-1) \rightarrow j}(W_j^l) \right)$$

correspond to infinitely many sequences of symbols in Ω_1 sharing the same central block, so this is a set of points exhibiting cycling of finite order m . Saturating this set by the flow we obtain a set of positive Lebesgue measure in the manifold.

Pick a finite sequence $\omega = z_1 \cdots z_m$ with $z_j \in \mathbf{N}$ and, without loss of generality, suppose its length is an integer multiple of k , i.e., $m = nk$, $n \in \mathbf{N}$. By the previous paragraph, there is a set of points whose trajectory exhibits cycling associated to this sequence. Concatenating infinitely many times the sequence ω , we obtain a periodic infinite sequence of natural numbers $(z_i)_{i \in \mathbf{Z}} \in \Omega_{\mathbf{N}}$ of period nk . Thus, $(1, (z_i)) \in \Omega^k$ is a fixed point of $(\sigma_*)^{nk}$. The point in $\Lambda_{\mathbf{N}}$ that corresponds to $(1, (z_i))$ has a periodic trajectory that exhibits finite cycling associated to the sequence ω . \square

From theorem 9 we also get:

Corollary 11. *For the dynamical system (Λ, G) , $k > 1$, defined in section 5.4, we have:*

- (1) *the topological entropy of (Λ, G) is $\log 2$;*
- (2) *(Λ, G) is topologically mixing, in particular (Λ, G) is topologically transitive and the set of periodic points of (Λ, G) is dense in Λ .*

Proof. (1) The topological entropy is invariant under conjugacy, thus by theorem 9 it is enough to show that (Ω_T, σ) has topological entropy $\log 2$.

The graph associated to T is strongly connected (it is possible to get from any vertex to any other by traversing a sequence of edges), therefore the matrix T is irreducible. Moreover, for each $j \in \{1, \dots, k\}$, the entries of any row of T^{k-1} correspond to permutations of the k elements of the line k of Pascal's Triangle, thus it follows that T is aperiodic.

Since T is irreducible and aperiodic, by the Perron-Frobenius theorem, its topological entropy h_{top} satisfies $h_{top} = \log(\lambda)$ where λ is the spectral radius of T (see Katok *et al* [22] and Kitchens [23] for details). Developing $\det(T - \lambda I)$ along the k -th row, we have

$$P(\lambda) = \det(T - \lambda I) = (-1)^{k+1} + (1 - \lambda)(1 - \lambda)^{k-1} = (-1)^{k+1} + (1 - \lambda)^k.$$

Hence $P(2) = 0$ and 2 is the real number with largest absolute value satisfying $P(\lambda) = 0$. Thus, $h_{top} = \log(2)$.

(2) By Katok & Hasselblatt (proposition 1.9.9 of Katok *et al* [22]), since the matrix T is aperiodic, the dynamical system (Ω_T, σ) is topologically mixing and its periodic orbits are dense in Ω_T . The result follows by conjugacy. \square

Roughly speaking, the topological entropy is a single positive number that represents the exponential growth rate of the total number of orbit segments distinguishable with arbitrarily fine but finite precision and it describes the exponential complexity of the orbit structure. Corollary 11 shows that if a cycle Σ whose nodes are periodic trajectories has more than two nodes, then the topological dynamics of (Λ, G) is of the same type for all $k > 1$, ie increasing the number of periodic nodes does not increase the number of statistically observable orbits near the cycle.

Theorem 9, together with the geometrical information of section 4, provides information on additional heteroclinic connections, as follows:

Proposition 12. *Let $\Sigma = \langle c_1, \dots, c_k \rangle$ be a heteroclinic cycle of hyperbolic periodic trajectories in a 3-dimensional manifold such that the invariant manifolds of consecutive nodes of Σ meet transversely. Then:*

- (1) *The trajectories c_1, \dots, c_k are the nodes of a heteroclinic network with all-to-all coupling, including homoclinic connections. Each pair of nodes is connected by a countable infinite set of trajectories.*
- (2) *At each heteroclinic connection the invariant manifolds of consecutive nodes meet transversely. Two different heteroclinic connections between the same pair of nodes are distinguished by the number of loops they make around the nodes in the cycle.*
- (3) *Points lying in heteroclinic connections are dense in Λ .*
- (4) *Σ is not asymptotically stable.*

Proof. (1) In the coding of section 5.4, a sequence $(z_i)_{i \in \mathbf{Z}} \in \Omega_T$ with z_i constant and equal to j for all $i > p$ corresponds to a point in the stable manifold of c_j and a sequence that is constant and equal to j for $i < p$ corresponds to a point in the unstable manifold of c_j . Thus, a sequence $(z_i)_i$ such that there exists $t_q < t_p \in \mathbf{Z}$ for which $\forall i < t_q, z_i = q$ and $\forall i > t_p, z_i = p$ codes a heteroclinic connection $[c_q \rightarrow c_p]$. Each central block from z_{t_q+1} to z_{t_p-1} corresponds to a different heteroclinic connection and the central block determines the number of turns around the nodes.

Note that the constant sequence $(z_i)_i$ such that $\forall i \in \mathbf{Z}, z_i = p$ corresponds to the node c_p of Σ , since any invariant saddle is contained in its stable and unstable manifolds.

- (2) For $k = 1$ the result is trivial. For $k \geq 2$, consider $m \in \{1, \dots, k\}$. Since the invariant manifolds of consecutive nodes in Σ intersect transversely, then locally $W^u(c_m) \cap H_{c_{m+1}}^{in}$ is a segment (in the terminology of section 4) near each intersection point. Its image by $\phi_{c_{m+1}}$ is a helix on $H_{c_{j+1}}^{out}$ accumulating on $W^u(c_{m+1})$. By transversality, there are infinitely many *arcs* of this helix, whose end points lie in $W^s(c_{m+2})$, which are mapped by $\Psi_{m+1 \rightarrow m+2}$ into segments on $H_{c_{m+2}}^{in}$. Each one of these segment is mapped into a helix on $H_{c_{m+2}}^{out}$ accumulating on $W^u(c_{m+2})$. This curve cuts $W^s(c_{m+3})$ transversely infinitely many times. It is possible to repeat the argument until, for any $n \in \{1, \dots, k\}$, the helix meets $W^s(c_n)$ infinitely many times. This helix corresponds to points of $W^u(c_m)$, hence, there exist infinitely many heteroclinic connections from c_m to c_n . It is possible to choose the heteroclinic connection from c_m to c_n turning around the nodes c_{m+1}, \dots, c_{n-1} any sequence of nonnegative numbers.
- (3) Pick $p \in \Lambda$ and let U be an open set such that $p \in U$. The image of U under the conjugacy ϑ is an open set corresponding to a set of sequences with the same central block X . Concatenating with a left infinite sequence of the type $\overleftarrow{a} = \dots aaa$ and with a right infinite sequence of the type $\overrightarrow{b} = bbb \dots$, the element $\overleftarrow{a} X \overrightarrow{b}$ belongs to $\vartheta(U)$ and corresponds to a heteroclinic connection from the saddle $\vartheta^{-1}(\dots aaa \dots)$ to the saddle $\vartheta^{-1}(\dots bbb \dots)$. The results follows immediately by conjugacy. It is worth noting that this holds for any choice of heteroclinic connection.
- (4) Trajectories starting close to an asymptotically stable heteroclinic cycle spend more and more time near each node on each visit. If Σ were asymptotically stable, then the times spent by a trajectory inside each of the neighbourhoods V_j would be a monotonically increasing sequence. This contradicts cycling because it is possible to find trajectories associated to any possible sequence of symbols. □

Theorem 9 may also be used to obtain a description of the behaviour of trajectories near the network of proposition 12.

Corollary 13. *Let $\Sigma = \langle c_1, \dots, c_k \rangle$ be a heteroclinic cycle of hyperbolic periodic trajectories in a 3-dimensional manifold such that the invariant manifolds of consecutive nodes of Σ meet transversely. Let Σ^* be a subnetwork of the network of proposition 12 such that Σ^* has finitely many hetero/homoclinic connections. Then there is switching near Σ^* . Moreover, we may prescribe the number of turns around each node for the trajectory that follows any sequence of connections. The combination of following a particular path and a given number of turns is realised by a unique trajectory.*

Thus, near the cycle Σ , there is a dense set corresponding to the transverse intersection of the invariant manifolds of different nodes, giving rise to a robust and transitive set with very rich persistent properties. The result is even more interesting due to the fact that the map F defined in 5.3 is uniformly hyperbolic in the intersection of $\Lambda_{\mathbf{N}}$ with any compact subset of $\mathcal{R}^{in,j}$, where it admits an invariant dominated

splitting, see Araújo and Pacifico [6]. The map G defined in 5.4 is uniformly hyperbolic at the points where it is defined and continuous.

7. CYCLING IN HIGHER DIMENSIONS

The results of the previous sections can be extended to higher dimensions using the centre manifold techniques of Homburg [19], Shaskov *et al* [40] and Shilnikov *et al* [41].

Consider a heteroclinic cycle Σ in \mathbf{R}^n whose nodes are hyperbolic periodic solutions c_j , $j = 1, \dots, k$ of $\dot{x} = f(x)$ with (possibly multiple) Floquet exponents $\lambda_i^j, 0, \gamma_i^j$, $i = 1, \dots, s$, $l = 1, \dots, u$, with $n = u + s + 1$, satisfying

$$\operatorname{Re}(\lambda_s^j) < \dots < \operatorname{Re}(\lambda_2^j) < \operatorname{Re}(\lambda_1^j) < 0 < \operatorname{Re}(\gamma_1^j) < \operatorname{Re}(\gamma_2^j) < \dots < \operatorname{Re}(\gamma_u^j).$$

Suppose the leading Floquet exponents λ_1^j and γ_1^j are both real and simple. Under these conditions, the results of Shilnikov *et al* [41] imply that generically there exists a smooth 3-dimensional flow-invariant centre manifold $W^c(\Sigma)$ that contains Σ .

We discuss briefly the genericity conditions and the properties of this manifold.

At each point p of c_j denote by E^{ss} , E^c and E^{uu} the subspaces associated to the Floquet exponents $\{\lambda_s^j, \dots, \lambda_2^j\}$, $\{\lambda_1^j, 0, \gamma_1^j\}$ and $\{\gamma_2^j, \dots, \gamma_u^j\}$, respectively. Besides the s -dimensional stable and u -dimensional unstable manifolds of c_j , there exists a centre unstable manifold $W^{cu}(c_j)$ that is tangent, at each point p of c_j , to the subspace $E^c \oplus E^{uu}$ and a centre stable manifold $W^{cs}(c_j)$ tangent to $E^{ss} \oplus E^c$. It is clear that $[c_j \rightarrow c_{j+1}] \subset W^{cu}(c_j) \cap W^{cs}(c_{j+1})$.

Shilnikov *et al* [41] proved that along $W^{cu}(c_j)$, there exists a u -dimensional strong unstable foliation \mathcal{F}^{uu} whose leaves at $p \in c_j$ include $W^{uu}(p)$. Similarly, along $W^{cs}(c_j)$ there exists an s -dimensional strong stable foliation \mathcal{F}^{ss} containing $W^{ss}(p)$ as a leaf at p . Both foliations are at least of class C^1 .

The genericity condition for existence of the centre manifold $W^c(\Sigma)$ is that at each point p of each heteroclinic connection, the centre unstable manifold $W^{cu}(c_j)$ is transverse to a leaf of \mathcal{F}^{ss} and $W^{cs}(c_{j+1})$ is transverse to a leaf of \mathcal{F}^{uu} . This condition avoids degenerate cases like the orbit flip, inclination flip, bellows and the homoclinic butterfly (see Homburg *et al* [21] for details).

On the centre manifold $W^c(\Sigma)$ the results of the preceding sections hold, so from Theorems 6, 9 and the results of Section 6 we get:

Theorem 14. *Let $\Sigma = \langle c_1, \dots, c_k \rangle$ be a heteroclinic cycle of hyperbolic non trivial periodic trajectories in a manifold of dimension $n \geq 3$ such that all c_j have the same number of Floquet exponents with negative real parts and the leading Floquet exponents are real and simple. If the invariant manifolds of consecutive nodes meet transversely, then, generically:*

- (1) Σ is contained in a smooth, flow-invariant, 3-dimensional center manifold $W^c(\Sigma)$;
- (2) Σ has finite and bi-infinite cycling;
- (3) there is a Cantor set Λ contained in $W^c(\Sigma)$ such that the first return map on Λ is conjugated to a subshift of finite type on k symbols;
- (4) Σ is not asymptotically stable neither in forward nor in backward time;
- (5) for each $j \in \{1, \dots, k\}$, there exist infinitely many homoclinic trajectories associated to c_j ;
- (6) if $k \geq 2$, for each $m, n \in \{1, \dots, k\}$, there exist infinitely many heteroclinic trajectories from c_m to c_n ;
- (7) for each $l \in \{2, \dots, k\}$ and each permutation $\sigma \in S_k$ of k elements there exists a heteroclinic network of periodic trajectories

$$\Sigma^{l\sigma} = \langle c_{\sigma(1)}, \dots, c_{\sigma(l)} \rangle.$$

whose invariant manifolds of consecutive nodes meet transversely.

8. CONSTRUCTION OF A HETEROCLINIC CYCLE BETWEEN THREE PERIODIC TRAJECTORIES IN A FIVE DIMENSIONAL SPHERE

In this section we construct a vector field in \mathbf{R}^6 for which our results may be applied. Restricted to a five dimensional invariant sphere it has a heteroclinic cycle between periodic trajectories and the invariant manifolds of two consecutive periodic trajectories intersect transversely. Thus, by the results above, the dynamics near the heteroclinic cycle exhibits chaotic cycling and all the associated dynamics.

The construction of the example relies on the technique presented in Aguiar *et al* [4] which consists essentially in three steps. In Aguiar *et al* [4], the authors start with a vector field on \mathbf{R}^3 with an attracting flow-invariant two-sphere containing a heteroclinic network. The heteroclinic network involves equilibria and one-dimensional heteroclinic connections that correspond to the intersection of fixed-point subspaces with the invariant sphere. The vector field needs to be at least \mathbf{Z}_2 -equivariant. Due to the \mathbf{Z}_2 -equivariance the vector field can be lifted by a rotation to a vector field on \mathbf{R}^4 with an attracting flow-invariant three-sphere. This forces some of the one-dimensional heteroclinic connections to become two-dimensional heteroclinic connections. The resulting vector field is $\mathbf{SO}(2)$ -equivariant. Finally, they perturb the vector field in a way that destroys the $\mathbf{SO}(2)$ -equivariance and such that the three-sphere remains invariant and globally attracting and some of the nontransverse two-dimensional heteroclinic connections perturb to transverse connections. Here we extend this procedure to three rotations.

This may be related to the construction in Melbourne [29] that starts with a $(\mathbf{Z}_2 \oplus \mathbf{Z}_2 \oplus \mathbf{Z}_2)$ -equivariant system of differential equations in \mathbf{R}^3 whose flow has an asymptotically stable heteroclinic network between six equilibria. Using this system as an amplitude equation and adding three phase equations, the system lifts to a flow in \mathbf{R}^6 that has now an asymptotically stable heteroclinic cycle between three periodic solutions with three-torus \mathbf{T}^3 symmetry. Each saddle of the cycle is what Krupa [25] calls a *relative equilibrium*. Adding a symmetry breaking term to the amplitude system breaks all the connections, the cycle disappears in the corresponding system in \mathbf{R}^6 , but any trajectory near the *ghost* of the cycle will reconstruct its shape. Melbourne estimated the quasi-period of trajectories near each periodic solution. In our approach, instead of perturbing the amplitude equations, we perturb the lifted vector field in \mathbf{R}^6 in such way that the heteroclinic cycle does not disappear and the invariant manifolds of consecutive nodes meet transversely.

We use the terminology of Aguiar *et al* [4], for results on dynamics. For symmetry, we refer the reader to Golubitsky *et al* [15].

8.1. Lifting a vector field. In Aguiar *et al* [4], it is proven how some properties of a \mathbf{Z}_2 -equivariant vector field in \mathbf{R}^3 lift by a rotation to properties of the resulting vector field in \mathbf{R}^4 . Those results generalize trivially to the lift by a rotation of a \mathbf{Z}_2 -equivariant vector field on \mathbf{R}^n to a vector field on \mathbf{R}^{n+1} . More concretely, let \mathbf{X}_n be a \mathbf{Z}_2 -equivariant vector field on \mathbf{R}^n . Without loss of generality, we can assume that \mathbf{X}_n is equivariant by the action

$$k_n(x_1, \dots, x_{n-1}, \omega) = (x_1, \dots, x_{n-1}, -\omega).$$

The vector field \mathbf{X}_{n+1} on \mathbf{R}^{n+1} is obtained by adding the auxiliary equation $\dot{\varphi}_n = 1$ and interpreting the coordinates (ω, φ_n) as polar coordinates. In rectangular coordinates (x_1, \dots, x_{n+1}) on \mathbf{R}^{n+1} , it corresponds to $x_n = \omega \cos \varphi_n$ and $x_{n+1} = \omega \sin \varphi_n$. The resulting vector field \mathbf{X}_{n+1} on \mathbf{R}^{n+1} is $\mathbf{SO}(2)$ -equivariant.

As in Aguiar *et al* [4], for $\Sigma \subset \mathbf{R}^n$ let $\mathcal{L}(\Sigma) \subset \mathbf{R}^{n+1}$ be the *lift by rotation* of Σ , the set of points (x_1, \dots, x_{n+1}) such that either (x_1, \dots, ω) or $(x_1, \dots, -\omega)$ lies in Σ , with $|\omega| = \|(x_n, x_{n+1})\|$. Consider the inclusion map $i_n : \mathbf{R}^n \rightarrow \mathbf{R}^{n+1}$, with

$$i_n(x_1, \dots, \omega) = (x_1, \dots, x_{n-1}, \omega, 0).$$

Extending the definition of heteroclinic connection between two invariant periodic solutions c_i and c_j as an m -dimensional connected flow-invariant manifold contained in $W^u(c_i) \cap W^s(c_j)$, the results in section 3 of Aguiar *et al* [4] generalize to:

Proposition 15. *Let \mathbf{X}_n be a $\mathbf{Z}_2(k_n)$ -equivariant vector field in \mathbf{R}^n and \mathbf{X}_{n+1} its lift to \mathbf{R}^{n+1} by rotation.*

- (a) *If $\Sigma \subset \mathbf{R}^n$ is invariant by the flow of \mathbf{X}_n , the $\mathcal{L}(\Sigma)$ is invariant by the flow of \mathbf{X}_{n+1} . In particular, if p is an equilibrium of \mathbf{X}_n then $\mathcal{L}(\{p\})$ is a relative equilibrium of \mathbf{X}_{n+1} .*
- (b) *If r_0 and r_1 are relative equilibria of \mathbf{X}_n and ξ is a k -dimensional connection from r_0 to r_1 , then:*
 - (1) *If ξ lies in $\text{Fix}(\mathbf{Z}_2(k_n))$, then r_0 and r_1 also lie in $\text{Fix}(\mathbf{Z}_2(k_n))$ and ξ lifts to a k -dimensional connection from the relative equilibria $i(r_0) = r_0$ to $i(r_1) = r_1$ of \mathbf{X}_{n+1} .*
 - (2) *If ξ is not contained in $\text{Fix}(\mathbf{Z}_2(k_n))$, then ξ lifts to a $(k+1)$ -dimensional connection from the relative equilibria $\mathcal{L}(r_0)$ to $\mathcal{L}(r_1)$ of \mathbf{X}_{n+1} .*
- (c) *If Σ is a compact \mathbf{X}_n -invariant asymptotically stable set then $\mathcal{L}(\Sigma)$ is a compact \mathbf{X}_{n+1} -invariant asymptotically stable set.*

- (d) If \mathbf{S}_r^{n-1} is an \mathbf{X}_n -invariant globally attracting sphere then $\mathcal{L}(\mathbf{S}_r^{n-1}) = \mathbf{S}_r^n$ is an \mathbf{X}_{n+1} -invariant globally attracting sphere.
- (e) If p is a hyperbolic equilibrium of \mathbf{X}_n then $\mathcal{L}(\{p\})$ is also hyperbolic.
- (f) The $\mathbf{SO}(2)$ -orbit of any \mathbf{X}_{n+1} -invariant set is always the lift of an \mathbf{X}_n -invariant set. In particular, any $\mathbf{SO}(2)$ -relative equilibrium of \mathbf{X}_{n+1} is the lift of an equilibrium of \mathbf{X}_n .

Moreover, it may be proved that if $\Sigma \subset \mathbf{R}^n$ is a compact flow-invariant set such that $\Sigma \subset \overline{W^s(\Sigma)} \setminus \Sigma$ and $\Sigma \subset \overline{W^u(\Sigma)} \setminus \Sigma$ then $\mathcal{L}(\Sigma)$ is also a compact flow-invariant set satisfying $\mathcal{L}(\Sigma) \subset \overline{W^s(\mathcal{L}(\Sigma))} \setminus \mathcal{L}(\Sigma)$ and $\mathcal{L}(\Sigma) \subset \overline{W^u(\mathcal{L}(\Sigma))} \setminus \mathcal{L}(\Sigma)$.

8.2. Construction of the example. Let $\Gamma \subset O(3)$ be the finite group generated by:

$$\begin{aligned} d(\rho_0, \rho_1, \rho_2) &= (\rho_1, \rho_2, \rho_0), \\ q(\rho_0, \rho_1, \rho_2) &= (-\rho_0, \rho_1, \rho_2). \end{aligned}$$

Let \mathbf{X}_3 be the fifth-order perturbation, studied in Aguiar [1], of the degree three normal form for the vector fields that are Γ -equivariant (see Guckenheimer *et al* [16]):

$$(4) \quad \begin{aligned} \dot{\rho}_0 &= \rho_0 (\lambda + \alpha\rho_0^2 + \beta\rho_1^2 + \gamma\rho_2^2 + \delta(\rho_1^4 - \rho_0^2\rho_2^2)), \\ \dot{\rho}_1 &= \rho_1 (\lambda + \alpha\rho_1^2 + \beta\rho_2^2 + \gamma\rho_0^2 + \delta(\rho_2^4 - \rho_0^2\rho_1^2)), \\ \dot{\rho}_2 &= \rho_2 (\lambda + \alpha\rho_2^2 + \beta\rho_0^2 + \gamma\rho_1^2 + \delta(\rho_0^4 - \rho_1^2\rho_2^2)). \end{aligned}$$

Theorem 16. For $\lambda > 0$, $\beta + \gamma = 2\alpha$, $\beta < \alpha < \gamma < 0$ and $\delta < 0$ the flow of the vector field \mathbf{X}_3 satisfies (see figure 9):

- (a) The sphere \mathbf{S}_r^2 , of radius $r = \sqrt{-\frac{\lambda}{\alpha}}$, is invariant by the flow and globally attracting.
- (b) The equilibria $p_0^\pm = (\pm r, 0, 0)$, $p_1^\pm = (0, \pm r, 0)$ and $p_2^\pm = (0, 0, \pm r)$ are hyperbolic saddles.
- (c) When restricted to the invariant sphere \mathbf{S}_r^2 the invariant manifolds of p_i^\pm , $i = 0, 1, 2$ satisfy:
 - (c.1) $W^u(p_i^\pm) \cap W^s(p_{i+1}^\pm) \pmod{3}$ is one-dimensional and
 - (c.2) $\cup_{i=0,1,2} [\{p_i^\pm\} \cup W^u(p_i^\pm)] = \cup_{i=0,1,2} [\{p_i^\pm\} \cup W^s(p_i^\pm)]$ is an asymptotically stable heteroclinic network with twelve connections between the saddles p_i^\pm .
- (d) Besides p_i^\pm , $i = 0, 1, 2$ and the origin, which is repelling, there are eight equilibria which are unstable foci on the restriction to \mathbf{S}_r^2 .

Proof. See the proof of Theorem 24 in Aguiar *et al* [1]. □

We use the procedure described in Section 2 of [4] to lift the three-dimensional vector field \mathbf{X}_3 , by three rotations, to a vector field in \mathbf{R}^6 . More specifically, since the vector field \mathbf{X}_3 is equivariant by the action $\mathbf{Z}_2(q) \oplus \mathbf{Z}_2(d^2qd) \oplus \mathbf{Z}_2(dqd^2)$, it has the form

$$\begin{aligned} \dot{\rho}_0 &= \rho_0 f(\rho_0^2, \rho_1^2, \rho_2^2), \\ \dot{\rho}_1 &= \rho_1 f(\rho_1^2, \rho_2^2, \rho_0^2), \\ \dot{\rho}_2 &= \rho_2 f(\rho_2^2, \rho_0^2, \rho_1^2), \end{aligned}$$

with $f : \mathbf{R}^3 \rightarrow \mathbf{R}$ such that

$$(5) \quad f(u_1, u_2, u_3) = (\lambda + \alpha u_1 + \beta u_2 + \gamma u_3 + \delta(u_2^2 - u_1 u_3)).$$

Adding the auxiliary equations $\dot{\varphi} = 1$, $\dot{\psi} = 1$ and $\dot{\sigma} = 1$ and interpreting each pair of coordinates (ρ_0, φ) , (ρ_1, ψ) and (ρ_2, σ) as polar coordinates, the vector field \mathbf{X}_3 lifts by three rotations to a vector field \mathbf{X}_6 on \mathbf{R}^6 of the form:

$$\begin{aligned} \dot{x}_1 &= x_1 f(x_1^2 + x_2^2, x_3^2 + x_4^2, x_5^2 + x_6^2) - x_2, \\ \dot{x}_2 &= x_2 f(x_1^2 + x_2^2, x_3^2 + x_4^2, x_5^2 + x_6^2) + x_1, \\ \dot{x}_3 &= x_3 f(x_3^2 + x_4^2, x_5^2 + x_6^2, x_1^2 + x_2^2) - x_4, \\ \dot{x}_4 &= x_4 f(x_3^2 + x_4^2, x_5^2 + x_6^2, x_1^2 + x_2^2) + x_3, \\ \dot{x}_5 &= x_5 f(x_5^2 + x_6^2, x_1^2 + x_2^2, x_3^2 + x_4^2) - x_6, \\ \dot{x}_6 &= x_6 f(x_5^2 + x_6^2, x_1^2 + x_2^2, x_3^2 + x_4^2) + x_5. \end{aligned}$$

Theorem 17. For the parameter values in theorem 16 the flow of the vector field \mathbf{X}_6 satisfies

- (C1) There is a five-dimensional sphere, \mathbf{S}_r^5 , that is invariant by the flow and globally attracting.

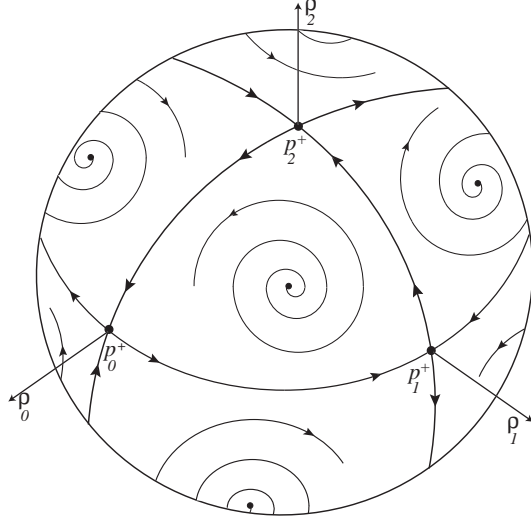


FIGURE 9. Heteroclinic network of the flow of the vector field \mathbf{X}_3 , restricted to the invariant sphere \mathbf{S}_r^2 . The intersection of the invariant sphere \mathbf{S}_r^2 with the invariant coordinate planes gives rise to three invariant circles. The union of these circles is the heteroclinic network whose existence is proved in theorem 17.

- (C2) *On the invariant five-sphere, there is an asymptotically stable heteroclinic cycle Σ with three periodic trajectories, c_i , $i = 0, 1, 2$. The invariant manifolds of the periodic trajectories satisfy, on the invariant sphere, $W^u(c_i) = W^s(c_{i+1}) \pmod{3}$, corresponding to three-dimensional heteroclinic connections.*
- (C3) *The origin is the only equilibrium and it is repelling.*
- (C4) *In the restriction to the invariant sphere \mathbf{S}_r^2 , there is a three-dimensional flow-invariant torus that is repelling.*

Proof. The proof relies on the results in proposition 15.

Number the rotations associated to the angular coordinates φ , ψ and σ as rotations 1, 2 and 3, respectively. The lift of the vector field \mathbf{X}_3 in \mathbf{R}^3 to the vector field \mathbf{X}_6 in \mathbf{R}^6 by the three rotations corresponds to a sequence of three lifts, by each of the three rotations.

Due to assertion (d) in proposition 15, since the sphere \mathbf{S}_r^2 is \mathbf{X}_3 -invariant and globally attracting, the sphere $\mathbf{S}_r^5 = \mathcal{L}(\mathbf{S}_r^4)$ is \mathbf{X}_6 -invariant and globally attracting.

Let $\Sigma_1 = \mathbf{Z}_2(q)$, $\Sigma_2 = \mathbf{Z}_2(d^2qd)$ and $\Sigma_3 = \mathbf{Z}_2(dqd^2)$. The fixed-point subspace $Fix(\Sigma_i) = \{(\rho_1, \rho_2, \rho_3) \in \mathbf{R}^3 : \rho_i = 0\}$, $i = 1, 2, 3$, is invariant by rotation i .

In the flow of \mathbf{X}_3 , the equilibria p_{i-1}^\pm , $i = 1, 2, 3$, lie in $Fix(\Sigma_{i+1}) \cap Fix(\Sigma_{i+2})$ and the heteroclinic trajectories connecting the equilibria p_{i-1}^\pm and p_i^\pm lie in $Fix(\Sigma_{i+2})$, $(\text{mod } 3)$. These, together with assertion (b) in proposition 15, prove the existence of the heteroclinic cycle Σ in assertion (C2).

More specifically, the equilibria p_{i-1}^\pm , $i = 1, 2, 3$, lift by rotation i to a periodic trajectory c_{i-1} , which remains invariant by the other two rotations. The periodic trajectory c_i , $i = 0, 1, 2$ has equations

$$x_{2i+1}^2 + x_{2i+2}^2 = r^2$$

and

$$x_{2i+3} = x_{2i+4} = x_{2i+5} = x_{2i+6} = 0 \pmod{6}.$$

By assertion (f) in proposition 15, the periodic trajectories c_i , $i = 0, 1, 2$, are hyperbolic.

The heteroclinic trajectories connecting equilibria p_{i-1}^\pm and p_i^\pm , $i = 1, 2, 3$, lift by rotation i to a pair of two-dimensional connections from the periodic trajectory c_{i-1} to the equilibria p_i^\pm . Then by rotation $i + 1$, they lift to a three-dimensional connection from the periodic trajectories c_{i-1} to c_i which remains invariant by rotation $i + 2$. The three-dimensional connection of the periodic trajectories c_{i-1} and c_i has equations

$$x_{2i+1}^2 + x_{2i+2}^2 + x_{2i+3}^2 + x_{2i+4}^2 = r^2$$

and

$$x_{2i+5} = x_{2i+6} = 0 \pmod{6}.$$

The asymptotic stability of the heteroclinic network in \mathbf{S}_r^2 and assertion (c) in proposition 15 imply the asymptotic stability of the heteroclinic cycle Σ in \mathbf{S}_r^5 .

Assertion (C4) follows from the existence of the eight unstable foci on \mathbf{S}_r^2 , that lie outside $Fix(\mathbf{Z}_2(q)) \cup Fix(\mathbf{Z}_2(d^2qd)) \cup Fix(\mathbf{Z}_2(dqd^2))$ and that their coordinates are

$$\left(\pm\sqrt{-\frac{\lambda}{3\alpha}}, \pm\sqrt{-\frac{\lambda}{3\alpha}}, \pm\sqrt{-\frac{\lambda}{3\alpha}} \right).$$

Thus, by rotation 1, they lift to four periodic trajectories, which lift to a pair of two-dimensional tori by rotation 2 and to a three-dimensional torus by rotation 3. Since the equilibria are repelling and due to assertion (e) in proposition 15 the torus is repelling.

By (e) and (f) in proposition 15 and assertions (d) and (e) in theorem 16 we obtain (C3). \square

Figure 10 corresponds to the time series of a trajectory in a neighbourhood of the asymptotically stable heteroclinic cycle in the flow of \mathbf{X}_6 . As in Melbourne [29], the trajectory starts near the periodic trajectory c_2 , spending some time nearby and jumps to the next periodic trajectory in the cycle, c_0 , staying there for a longer period of time. This kind of motion continues around the heteroclinic cycle before returning to the periodic trajectory c_2 . The asymptotic stability of the heteroclinic cycle implies that the sequence of times spent near the nodes is monotonically increasing.

Perturbation and transverse intersection of manifolds - numerical simulation. The vector field \mathbf{X}_6 is $\mathbf{Z}_3 \times \mathbf{SO}(2)^3$ -equivariant. The three-dimensional heteroclinic connections in Σ correspond to the intersection of the invariant sphere \mathbf{S}_r^5 with the fixed-point subspaces of the rotational symmetries. Moreover, on the the invariant sphere \mathbf{S}_r^5 they correspond to the nontransverse intersection of the invariant manifolds of the periodic trajectories. We now perturb \mathbf{X}_6 keeping \mathbf{S}_r^5 invariant while forcing those invariant manifolds to intersect transversely on one-dimensional heteroclinic connections between the periodic trajectories.

The perturbing term we consider is:

$$P(x_1, x_2, x_3, x_4, x_5, x_6) = \begin{pmatrix} x_4x_5x_6 \\ -x_3x_4x_5 \\ x_1x_2x_6 \\ -x_1x_5x_6 \\ x_2x_3x_4 \\ -x_1x_2x_3 \end{pmatrix}$$

and thus the perturbed vector field is $\mathbf{X}_6^p = \mathbf{X}_6 + \varepsilon P$, with ε small. Note that this perturbation is \mathbf{Z}_3 -equivariant. The perturbation keeps the invariance of the planes defined by

$$x_3 = x_4 = x_5 = x_6 = 0, \quad x_1 = x_2 = x_5 = x_6 = 0$$

and

$$x_1 = x_2 = x_3 = x_4 = 0$$

and is tangent to the invariant sphere; thus the invariant sphere and the three periodic trajectories are invariant by the perturbed flow. However, the perturbation breaks the invariance of the hyperplanes defined by $x_1 = x_2 = 0$, $x_3 = x_4 = 0$ and $x_5 = x_6 = 0$ that contain the heteroclinic connections and so the connections are perturbed.

Although we do not prove analytically that the invariant manifolds of consecutive periodic trajectories intersect transversely, this will generically be the case. Here, we intend to present some evidences of that, namely chaotic behaviour. High sensibility to initial conditions is emphasized in figures 11, 12 and 13. Figures 11 and 12 show the abrupt x_i -variation of two trajectories having started very close. Figure 12 claims also the existence of chaotic cycling. The simulations in figures 11 and 12 show evidence of instant chaos near the perturbed heteroclinic cycle due to the explosion of suspended horseshoes and homoclinic classes.

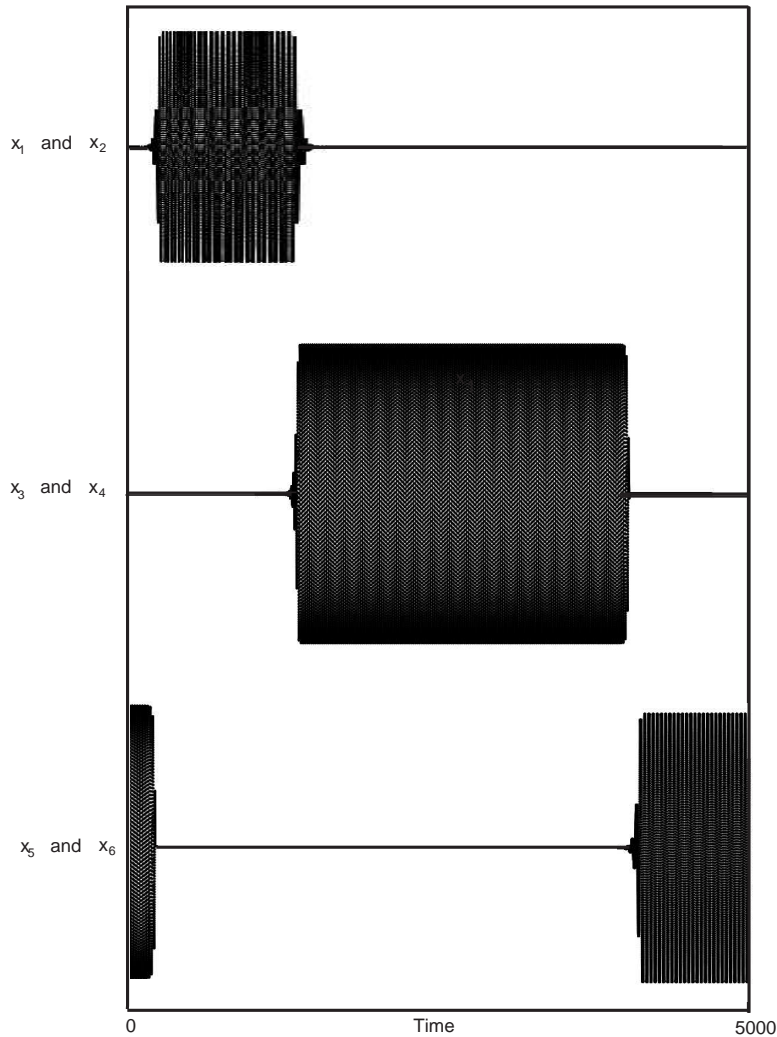


FIGURE 10. Time series corresponding to a solution near the asymptotically stable heteroclinic cycle in the flow of the vector field \mathbf{X}_6 , with $\lambda = 1$, $\alpha = -0.33333333$, $\beta = -0.5$, $\gamma = -0.16666667$ and $\delta = -0.05$. The initial condition is $(0.500, -0.05, -0.500, -0.500, 0.500, -0.500)$.

Bifurcating to chaos. As we know from the previous sections, for $\varepsilon \neq 0$, there is a infinite number of heteroclinic and homoclinic connections between any two periodic trajectories and the dynamics near the heteroclinic network is very complex. As we have seen using symbolic dynamics, the set of homo and heteroclinic connections near the perturbed cycle is dense in the set of nonwandering trajectories of the cycle. As $\varepsilon \rightarrow 0$, the infinity of connections tend to the two dimensional connections between consecutive periodic trajectories that exist for $\varepsilon = 0$, and the remaining cycle becomes asymptotically stable, attracting all trajectories in a small neighbourhood.

This phenomenon is a consequence of the symmetry breaking and the route to the chaos corresponds to a curious interaction between symmetry breaking, robust switching and chaotic cycling. This dynamical phenomenon is even more interesting because of the emergence of chaotic cycling (after perturbation) do not depend on the magnitude of the multipliers of the periodic trajectories. It only depend on the geometry of the flow near the cycle. The magnitude of the multipliers is only crucial to study the stability of the unperturbed cycle.

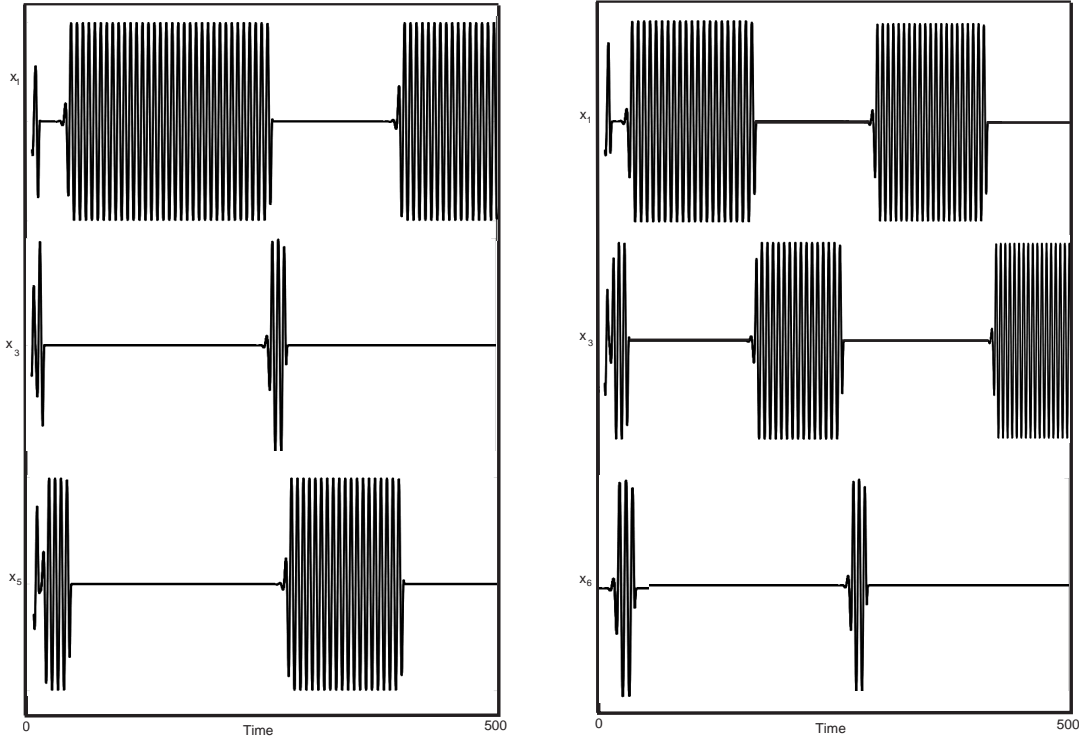


FIGURE 11. Time series for two trajectories with close initial condition for the flow corresponding to the vector field $\mathbf{X}_6 + \varepsilon P$, with $\lambda = 1$, $\alpha = -0.33333333$, $\beta = -0.5$, $\gamma = -0.16666667$, $\delta = -0.05$ and $\varepsilon = 1$ (the same trajectories as in figure 12). Left: the initial condition is $(-1.089, 1.715, -0.5, -0.5, 0.406, -0.5)$; Right: the initial condition is $(-1.090, 1.715, -0.5, -0.5, 0.407, -0.5)$. These time series illustrate the cycling of finite order.

Lyapunov exponents. One of the most efficient tools for the study of chaotic dynamical systems is the computation of the Lyapunov Exponents. Roughly speaking, they measure the stability and instability of trajectories under perturbation. For \mathbf{X}_6^p and $\lambda = 1$, $\alpha = -0.33333333$, $\beta = -0.5$, $\gamma = -0.16666667$ and $\delta = -0.05$, one of the Lyapunov Exponents is $0,00055 > 0$. By Oseledets' Theorem, this means that there exists x and $v \in T_x \mathbf{S}^5$ such that

$$\|D_x F^n(v)\| > 1,$$

where F is the first return map near the heteroclinic cycle. Thus, v grows exponentially at a rate $0,00055$ in the future and contract exponentially at the same rate in the past. In our setting, it shows that P corresponds to a unstable perturbation, illustrating that the distant future is practically inaccessible and may only be described in average, in probabilistic and ergodic terms. Since, on a large scale, the evolution resembles a random process, the symbolic dynamics used in sections 5.3 and 5.4 will be a very helpful tool to tackle the complete characterization of this network.

ACKNOWLEDGEMENTS

The authors are grateful to D. Turaev and W. S. Koon for helpful comments, to Oksana Koltsova from the Imperial College of London for helpful discussions and to Murilo S. Baptista for the numerical computation of the Lyapunov exponents. The first author thanks to Jeroen Lamb for the hospitality at the Imperial College of London.

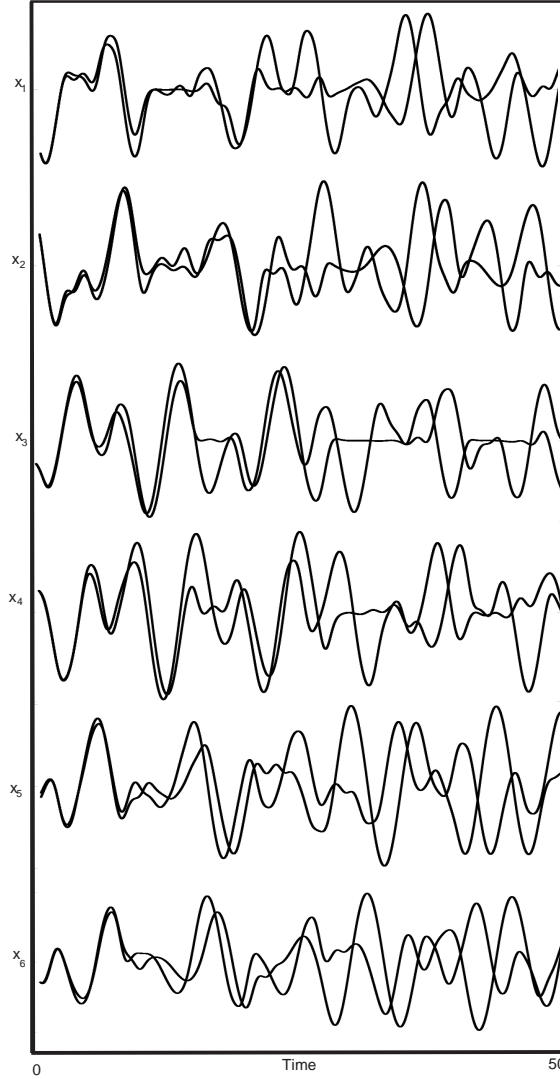


FIGURE 12. Time series for two trajectories with close initial condition for the flow corresponding to the vector field $\mathbf{X}_6 + \varepsilon P$, with $\lambda = 1$, $\alpha = -0.33333333$, $\beta = -0.5$, $\gamma = -0.16666667$, $\delta = -0.05$ and $\varepsilon = 1$ (the same trajectories as in figure 11). Left: the initial condition is $(-1.089, 1.715, -0.5, -0.5, 0.406, -0.5)$; Right: the initial condition is $(-1.090, 1.715, -0.5, -0.5, 0.407, -0.5)$. Note that the two time series are different, illustrating the *high* sensitivity to initial conditions.

APPENDIX A. ESTIMATES OF CONTRACTION RATES ON STRIPS

Lemma 18. *If U is a vertical strip of width d across $\mathcal{R}^{in,j}$ and $m \geq 1$, then $P_j(m, U)$ is a vertical strip across $\mathcal{R}^{in,j+1}$ of width $D \leq \mu_m d$, where*

$$\mu_m = \varepsilon C_j e^{-2\pi C_j(m-1)}.$$

If W is a vertical strip of width d across $\mathcal{R}^{out,j}$ and $m \geq 1$, then $Q_j(m, W)$ is a vertical strip across $\mathcal{R}^{out,j-1}$ of width $D \leq \nu_m d$, where

$$\nu_m = \varepsilon E_j e^{-2\pi E_j m}.$$

Proof. We only prove the assertion about $P_j(m, U)$ since the proof for $Q_j(m, W)$ is quite similar, with appropriate adaptations. By corollary 7, if U is a vertical strip across $\mathcal{R}^{in,j}$ then $\widehat{U} = \phi_{c_j}(U \cap \overline{\mathcal{I}_j^m})$ is

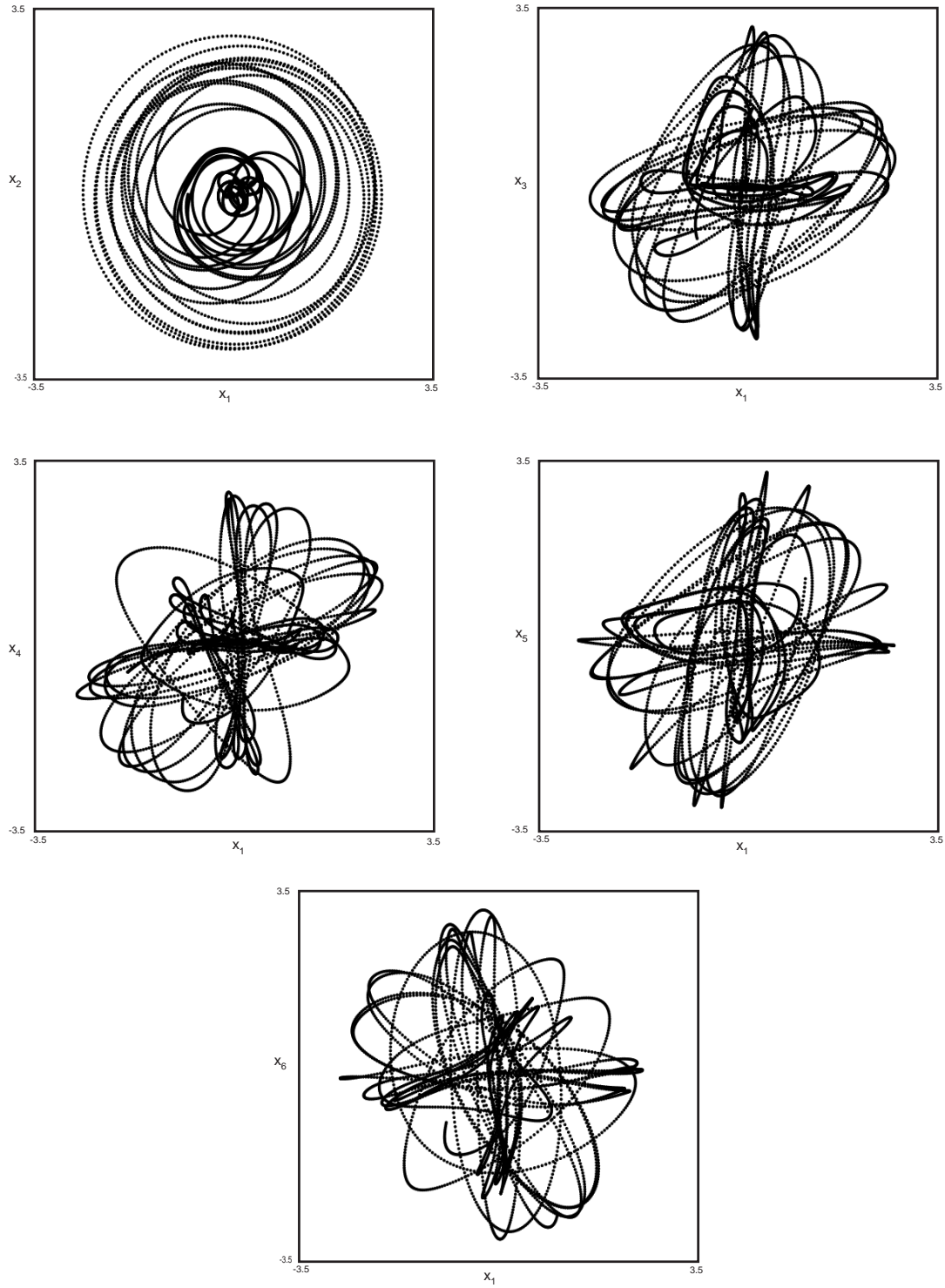


FIGURE 13. Projection in the (x_1, x_2) , (x_1, x_3) , (x_1, x_4) , (x_1, x_5) and (x_1, x_6) planes of the trajectory with initial condition $(-1.089, 1.715, -0.500, -0.500, 0.406, -0.5)$ for the flow corresponding to the vector field $\mathbf{X}_6 + \varepsilon P$, with $\lambda = 1$, $\alpha = -0.33333333$, $\beta = -0.5$, $\gamma = -0.16666667$, $\delta = -0.05$ and $\varepsilon = 1$.

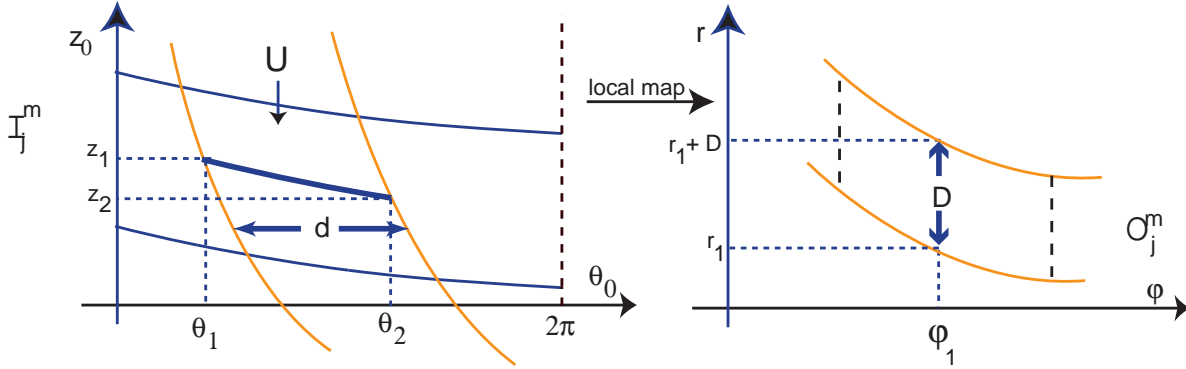


FIGURE 14. By corollary 7, for $m \in \mathbb{N}$ the set $\widehat{U} = \phi_{c_j}(U \cap \overline{\mathcal{I}_j^m})$ is a horizontal strip across the width of $H_{c_j}^{out}$ and thus $\widehat{U} \cap \mathcal{R}^{out,j}$ is a horizontal strip.

a horizontal strip across $\mathcal{R}^{out,j}$, which is mapped by $\Psi_{j \rightarrow j+1}$ into a vertical strip across $\mathcal{R}^{in,j+1}$. For these estimates we make the simplifying assumption that $\Psi_{j \rightarrow j+1}$ is a rotation of $\pi/2$ around $(A, 1)$ followed by a translation mapping $(A, 1)$ to $(B, 0)$. Without this assumption the estimates hold with all the μ_m multiplied by a suitable constant. Thus, the width D that we want to estimate is the height of $\widehat{U} = \phi_{c_j}(U \cap \overline{\mathcal{I}_j^m})$. This height is the length of a segment connecting two points with the same angular coordinate (see figure 14). Let (φ_1, r_1) and $(\varphi_1, r_1 + D)$ be these points and denote their pre-image under ϕ_{c_j} by (θ_1, z_1) and (θ_2, z_2) , respectively, with $\theta_1, \theta_2 \in [0, 2\pi]$.

From the expression (3) for ϕ_{c_j} given in section 3, it follows that since the angular coordinates of $\phi_{c_j}(\theta_1, z_1)$ and $\phi_{c_j}(\theta_2, z_2)$ are equal, then:

$$\theta_1 - \frac{1}{E_j} \ln \left(\frac{z_1}{\varepsilon} \right) = \theta_2 - \frac{1}{E_j} \ln \left(\frac{z_2}{\varepsilon} \right)$$

which is equivalent to:

$$z_2 = z_1 e^{E_j(\theta_2 - \theta_1)}.$$

Since $\phi_{c_j}(\theta_1, z_1)$ and $\phi_{c_j}(\theta_2, z_2)$ lie in the same vertical segment of length D , this means that:

$$1 + \varepsilon \left(\frac{z_2}{\varepsilon} \right)^{\frac{C_j}{E_j}} = 1 + \varepsilon \left(\frac{z_1}{\varepsilon} \right)^{\frac{C_j}{E_j}} + D.$$

and therefore

$$(6) \quad \frac{D}{\varepsilon} = \left(\frac{z_1}{\varepsilon} \right)^{\frac{C_j}{E_j}} \left(e^{C_j(\theta_2 - \theta_1)} - 1 \right).$$

Since (θ_1, z_1) and (θ_2, z_2) lie inside the strip \mathcal{I}_j^m , we have:

$$2\pi m \leq \theta_1 - \frac{1}{E_j} \ln \left(\frac{z_1}{\varepsilon} \right) \leq 2\pi(m+1)$$

and thus it follows that:

$$E_j(-2\pi(m+1) + \theta_1) \leq \ln \left(\frac{z_1}{\varepsilon} \right) \leq E_j(-2\pi m + \theta_1)$$

giving rise to:

$$(7) \quad e^{-2\pi(m+1)E_j} e^{\theta_1 E_j} \leq \frac{z_1}{\varepsilon} \leq e^{-2\pi m E_j} e^{\theta_1 E_j}.$$

From the second inequality of (7), we may conclude that:

$$(8) \quad \frac{z_1}{\varepsilon} \leq e^{-2\pi m E_j} e^{\theta_1 E_j} \leq e^{-2\pi m E_j} e^{2\pi E_j} = e^{-2\pi E_j(m-1)}$$

Substituting (8) into (6), and taking into account that $\theta_2 - \theta_1 \leq d$ (since the width of U is d), we show that

$$\frac{D}{\varepsilon} \leq e^{-2\pi C_j(m-1)} \left(e^{C_j(\theta_2 - \theta_1)} - 1 \right) \leq e^{-2\pi C_j(m-1)} (C_j d + |o(d^2)|)$$

with a positive remainder $|o(d^2)|$ and hence $D \leq \varepsilon C_j d e^{-2\pi C_j(m-1)}$. □

REFERENCES

- [1] M. A.D. Aguiar. Vector fields with heteroclinic networks, *Phd thesis, Departamento de Matemática Aplicada, Faculdade de Ciências da Universidade do Porto* (2003).
- [2] M. Aguiar, P. Ashwin, A. Dias and M. Field, *Dynamics of coupled cells systems: synchrony, heteroclinic cycles and inflation*, CMUP preprint 2009 (<http://www.fep.up.pt/docentes/maguiar>)
- [3] M. Aguiar, S. B. Castro and I. S. Labouriau, *Dynamics near a heteroclinic network*, *Nonlinearity* 18, 2005
- [4] M. A. D. Aguiar, S. B. S. D. Castro and I. S. Labouriau. *Simple Vector Fields with Complex Behavior*, *Int. Jour. of Bif. and Chaos*, Vol. **16** No. **2**, 2006
- [5] M. A. D. Aguiar, I. S. Labouriau and A. A. P. Rodrigues, *Switching near a heteroclinic network of rotating nodes*, *Dynamical Systems: an International Journal*, Vol. 25, Issue 1, 2010
- [6] V. Araújo and M. J. Pacifico, *Three-Dimensional Flows*, Vol 53 of *Ergebnisse der Mathematik und ihrer Grenzgebiete*, Springer, 2010
- [7] D. Armbruster, J. Guckenheimer and P. Holmes, *Heteroclinic cycles and modulated travelling waves in systems with $O(2)$ symmetry*, *Physica D*, No. **29**, 1988
- [8] P. Ashwin and M. Field, *Heteroclinic Networks in Coupled Cell Systems*, *Arch. Rational Mech. Anal*, 1999
- [9] G. D. Birkhoff, *Dynamical Systems*, A.M.S. Collection Publication, **9**, American Mathematical Society: Providence, 1927 (reprinted 1966)
- [10] G. D. Birkhoff, *Nouvelles recherches sur les systèmes dynamiques* *Mem. Pont. Acad. Sci. Novi. Lyncaei*, No. **1**, 1935
- [11] P. Ashwin, M. Field, A.M. Rucklidge and R. Sturman, *Phase resetting effects for robust cycles between chaotic sets*, *Chaos* 13, 2003
- [12] L. Barreira, G. Iommi, *Suspension Flows Over Countable Markov Shifts*, *Journal of Statistical Physics*, Volume 124, No. **1**, 2006
- [13] M. Dellnitz, M. Field, M. Golubitsky, A. Hohmann and J. Ma, *Cycling Chaos*, *IEEE Transactions on Circuits and Systems. 1. Fundamental Theory and Applications*, Vol. **42**, No. **10**, 1995
- [14] M. Field, *Lectures on bifurcations, dynamics and symmetry*, *Pitman Research Notes in Mathematics Series*, Vol. **356**, Longman, 1996
- [15] M. I. Golubitsky, I. Stewart, and D. G. Schaeffer, *Singularities and Groups in Bifurcation Theory*, Vol. **II**, Springer, 2000
- [16] Guckenheimer, J. & Holmes, P., *Structurally stable heteroclinic cycles*, *Math. Proc. Camb. Phil. Soc.*, No. **103**, 1988
- [17] J. Hadamard, *Les surfaces à courbures opposés et leurs lignes géodésiques*, *Journal de Mathématiques*, **5**, 1898
- [18] P. Hartman, *On local homeomorphisms of Euclidean spaces*, *Bol. Soc. Mexicana*, No. **5**, pages 220-241
- [19] A. J. Homburg, *Global Aspects of Homoclinic Bifurcations in Vector Fields*, *Memoirs of the American Mathematical Society*, No. **578**, Vol. **121**, American Mathematical Society, 1996
- [20] A. J. Homburg and J. Knoblock, *Multiple Homoclinic Orbits in Conservative and Reversible Systems*, *Transactions of the American Mathematical Society*, Vol. **358**, No. **4**, 2005
- [21] A. J. Homburg and B. Sandstede, *Homoclinic and Heteroclinic Bifurcations in Vector Fields*, *Handbook of Dynamical Systems III* (to appear), 2009
- [22] A. Katok, B. Hasselblatt, *Introduction to the Modern Theory of Dynamical Systems*, Cambridge University Press, 1995
- [23] Kitchens, B.P., *Symbolic Dynamics*, Springer, 1998
- [24] W. S. Koon, M. Lo, J. Marsden, S. Ross, *Heteroclinic Connections between Periodic Orbits and Resonance Transition in Celestial Mechanics*, *Control and Dynamical Systems Seminar* (California Institute of Technology), 1999
- [25] M. Krupa, *Bifurcations of relative equilibria*, *SIAM J. Math. Anal.*, Vol **21**, No. **6**, 1990
- [26] M. Krupa, *Robust Heteroclinic Cycles*, *J. Nonlinear Sci.*, No. **7**, 1997
- [27] M. Krupa and I. Melbourne, *Asymptotic Stability of Heteroclinic Cycles in Systems with Symmetry, II*, *Proc. Roy. Soc. Edinburgh*, No. **134A**, 2004
- [28] J. S. W. Lamb, M. A. Teixeira and Kevin N. Webster, *Heteroclinic bifurcations near Hopf-zero bifurcation in reversible vector fields in \mathbf{R}^3* , *Journal of Differential Equations*, No. **219**, 2005
- [29] I. Melbourne, *Intermittency as a Codimension-Three Phenomenon*, *Journal of Dynamics and Differential Equations*, No. **4**, 1989
- [30] I. Melbourne, M. R. E. Proctor and A. M. Rucklidge, *A heteroclinic model of geodynamo reversals and excursions*, 2001

- [31] R. Moeckel, *Chaotic Orbits in the Three Body Problem*, in P.H. Rabinowitz, A. Ambrosetti, I. Ekeland and E.J. Zehnder (eds.) *Periodic Solutions of Hamiltonian Systems and Related Topics (Il Ciocco 1986)* NATO ASI Ser. C 209, Reidel, Dordrecht, 1987
- [32] M. Morse and G. A. Hedlund, *Symbolic Dynamics*, American Journal of Mathematics, **60**, 1938
- [33] J. Moser, *Stable and Random Motions in Dynamical Systems*, Princeton University Press, 1973
- [34] A. Palacios, *Heteroclinic cycles in coupled systems of difference equations*, Journal of Difference Equations and Applications 9, No. **7**, 2002
- [35] A. Palacios, H. Juarez, *Cryptography with Cycling Chaos*, Physics Letters A, Vol. **303**, Issues 5-6, 2002
- [36] A. Palacios and P. Longhini, *Cycling behavior in near-identical cell systems*, International Journal of Bifurcation and Chaos, 13, No. **9**, 2003
- [37] C. M. Postlethwaite and J. H. P. Dawes, *Regular and irregular cycling near a heteroclinic network*, Nonlinearity, Vol. **18**, 2005
- [38] O. Sarig, *Thermodynamic Formalism for Countable Markov Shifts*, Ergodic Th. Dynam. Sys., No. **19**, 1999
- [39] M. A. Savi, *Chaos and Order in Biomedical Rhythms*, J. of the Braz. Soc. of Mech. Sci. & Eng, Volume XXVII, No. **2**, 157, 2005
- [40] M. Shashkov, D. V. Turaev, *An Existence Theorem of Smooth Nonlocal Center Manifolds for Systems Close to a System with a Homoclinic Loop*, J. Nonlinear Sci., Vol. **9**, 1999
- [41] Shilnikov, L.P., Shilnikov, A. L., Turaev, D. M. and Chua, L. U., *Methods of Qualitative Theory in Nonlinear Dynamics*, Part I, World Scientific Publishing Co., 1998
- [42] S. Smale, *Diffeomorphisms with many periodic points*, Differential and Combinatorial Topology (A Symposium in Honor of Marston Morse), Princeton Univ. Press, Princeton, N.J., 1965
- [43] S. Wiggins, *Global Bifurcations and Chaos: Analytical Methods*, Springer-Verlag, 1988
- [44] S. Wiggins, *Introduction in Applied Nonlinear Dynamical Systems and Chaos*, Springer-Verlag, TAM 2, 1990

(I.S. Labouriau and A.A.P. Rodrigues) CENTRO DE MATEMÁTICA DA UNIVERSIDADE DO PORTO, AND FACULDADE DE CIÊNCIAS DA UNIVERSIDADE DO PORTO, RUA DO CAMPO ALEGRE 687, 4169-007 PORTO, PORTUGAL

E-mail address, A.A.P.Rodrigues: alexandre.rodrigues@fc.up.pt

E-mail address, I.S.Labouriau: islabour@fc.up.pt

(M.A.D.Aguiar) CENTRO DE MATEMÁTICA DA UNIVERSIDADE DO PORTO, AND FACULDADE DE ECONOMIA DA UNIVERSIDADE DO PORTO, RUA DR. ROBERTO FRIAS, 4200-464 PORTO, PORTUGAL

E-mail address: maguiar@fep.up.pt